Materials Today Chemistry 36 (2024) 101926

Contents lists available at ScienceDirect

Materials Today Chemistry

journal homepage: www.journals.elsevier.com/materials-today-chemistry/

Review on composite polymer electrolyte using PVDF-HFP for solid-state lithium-ion battery

Bhargabi Halder [a], Mohamed Gamal Mohamed [b,c], Shiao-Wei Kuo [b], Perumal Elumalai [a,*]

[a] Electrochemical Energy Storage Lab, Department of Green Energy Technology, Madanjeet School of Green Energy Technologies, Pondicherry University, Puducherry, 605014, India

[b] Department of Materials and Optoelectronic Science, College of Semiconductor and Advanced Technology Research, Center for Functional Polymers and Supramolecular Materials, National Sun Yat-Sen University, Kaohsiung, 804, Taiwan

[c] Chemistry Department, Faculty of Science, Assiut University, Assiut, 71515, Egypt

ARTICLE INFO

Keywords:
Solid-state battery
Composite polymer electrolytes
Passive-active fillers
Ionic conductivity
Electrode-electrolyte interface

ABSTRACT

Solid-state lithium-ion batteries with composite polymer electrolytes are considered to be one of the most apparent technology to lead in the world of batteries. The primary upside of such batteries is their addressed safety issues followed by good flexibility along with mechanical strength and improved interfacial conditions. Among various polymers, poly (vinylidene fluoride-hexafluoropropylene) (PVDF-HFP) has exhibited to be potential enough to easily dissociate lithium salts as it is enriched with strong electron withdrawing groups. Along the years, researchers have introduced various methods by which the ionic conductivity and the overall performance have effectively improved. Hence, in this review we briefly discuss the recent progress and major contributions of several passive and active fillers in composite polymer electrolytes (CPEs) and how they consequently impact the overall cell performance. The unique mechanisms as well as effects of fillers with respect to their dimension, optimal quantity and type and how they can overcome the limitations of conventional solid polymer electrolytes (SPEs) are detailed here. Mostly the factors affecting the ionic conductivity and overall cell performance in PVDF-HFP based CPEs are intensively reviewed. Finally, we evaluated the improvisions made to diminish the electrode-electrolyte interfacial resistance which contributes a major role in all solid-state batteries.

1. Introduction

Currently energy demand exponentially increases due to pronounced growth of industries, huge hike in fossil fuel utilization for transportation, increasing human population, extensive usage of modern electronic gadgets, etc. At this stage, there is no feasible way to actually decline the consumption of energy, rather we should focus on how to effectively use the energy that is generated or the energy which is available on the Earth's crust and is viable for use of humans [1,2]. Major efforts are aimed at development of energy storage devices such as supercapacitors and batteries to effectively hold the energy that is generated for future use. The relying on the use of renewable energy is not a solution to this abruptly increasing energy demand as it is reported that the global consumption of renewable energy will reach 247 EJ by 2050 [3] as the renewable energy is geological region specific as well as time specific and cannot be harvested equally throughout all regions. Thereby, the sole effective way of moving forward is to store the energy generated in potent and highly efficient energy storage devices [4]. Lithium-ion batteries (LIBs) have been ruling the market over three decades since Sony and Asahi Kasei first commercially marketed it in 1991 [5]. Ever since, it has made an accelerated growth in the development of its electrode materials as well as its electrolytes. Till date, a conventionally commercial LIB comprises of an anode at the left terminal where oxidation (insertion of Li^+) takes place along with a cathode at the right terminal where reduction (re-insertion of Li^+) takes place along with a separator in between accompanied with an organic electrolyte containing Li^+ conducting salts [6,7]. It has been ruling the market since three decades as it is utilized in electronic gadgets, consumer electronic appliances, electric vehicles, etc., due to its superior voltage and high capacity leading to high energy densities [8]. The major drawback of such batteries is the safety concern that holds them back to a certain extent despite of the excellent wettability on the electrode surface and fulfilling ionic conductivity on a commercial level [9]. To dig into the problems of major accidents caused by the liquid

* Corresponding author.
E-mail addresses: drperumalelumalai@pondiuni.ac.in, drperumalelumalai@gmail.com (P. Elumalai).

https://doi.org/10.1016/j.mtchem.2024.101926
Received 21 October 2023; Received in revised form 22 December 2023; Accepted 13 January 2024
Available online 23 January 2024

electrolyte-based LIB due to buildup of heat leading to explosions or electrolyte leakage due to the volume consumed by it, the development of solid-state batteries has become a word of change here [10]. The usage of lithium metal as the anode in the conventional batteries is hindered as lithium metal is prone to form dendrites in the liquid electrolytes leading to detrimental effects which thereby restricts the energy density to slide up [12]. In a solid-state battery, the volume advantage is one factor that is addressed along with the prime concerns of flammability and dendrite formation which are effectively being rectified [13]. Nevertheless, the issues of interfacial resistance and moderately low ionic conductivity at room temperature hinder them in implementing for the commercial market [14]. Looking at the upside, the solid-state batteries have better thermal as well as mechanical stability and also a steady conduction of lithium ion for unvaried deposition on the anode, leading it to achieve increased stability during long cycling of the desired cell [15]. Fig. 1 depicts the schematic representation of the evolved LIBs over extensive research to achieve higher energy density. Solely, the solid-state batteries are of different kinds using mainly three types of solid electrolytes i.e., inorganic or ceramic solid electrolytes (ISEs), solid polymer electrolytes (SPEs) and composite polymer electrolytes (CPEs) [16]. Inorganic solid electrolytes are purely crystalline in nature and tend to have high interfacial resistance due to irregular electrode surfaces and lack of contact between electrolyte and electrode. As they are mechanically rigid, they can withstand the dendrites of metallic lithium. On the other hand, SPEs are made of polymers or polymer blends or crosslinking along with easily dissociable lithium salts. They are mostly not functional at room temperature due to lack of acceptable ionic conductivity range. It is to be noted that due to flexibility of polymers they have lower interfacial resistance but cannot withstand the puncture of lithium metal dendrites due to insufficient mechanical strength [17]. Also, the tapered stable electrochemical window and lower lithium-ion transference number than the ceramic solid electrolyte hinders its practical acceptance. Therefore, after quite research advancement, CPEs have come in the way which comprises of both the above-mentioned electrolytes to achieve better cell performance [18]. In comparison to the liquid electrolytes, there is still a shortfall on the ionic conductivity of the CPE with improved safety concern, weight as well as large volume decrease. The CPEs can be used not only in lithium-ion batteries but also in all battery systems that use

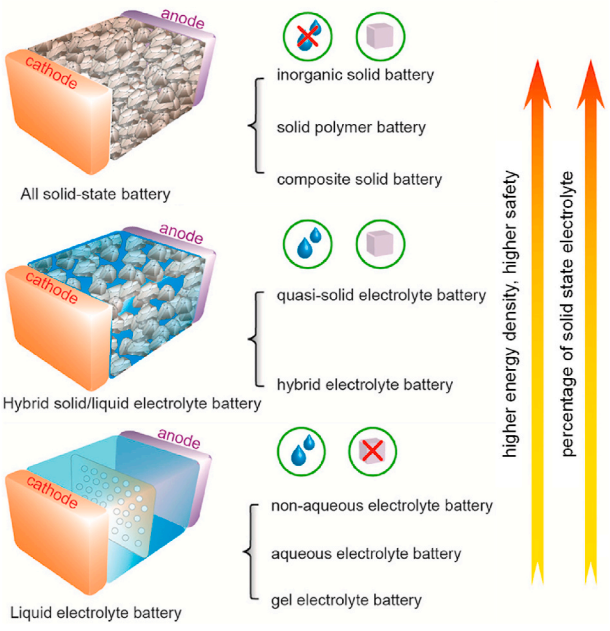

Fig. 1. Schematic representation of the existing lithium-ion batteries on basis of various electrolytes. Adapted with permission from ref. [11].

lithium metal as an electrode like Li–S, Li–O_2, Li–Se, Li–CO_2 batteries because lithium metal is capable of offering a very high theoretical capacity of 3860 mA h g^{-1} and electrochemical potential as low as −3.04 V vs SHE, and also light weight as its atomic mass is 6.941 amu [19–22]. Diving into the literature of the various solid-state electrolytes, ISE possess a purely robust nature of its own and are highly compatible with cathodes of high voltages to give enhanced energy densities [23]. They are broadly classified into oxide-based electrolytes and sulfide-based electrolytes. Oxide-based electrolytes such as garnet-type, perovskite-type, NASICON-type oxides, etc are widely explored [24–26]. They impart a moderate range of ionic conductivity in between those of sulfides and solid polymer electrolytes and are the most compatible with lithium metal at the interface having high mechanical and electrochemical stability towards Li [27]. Unfortunately, oxides are more on the brittle end as compared to sulfide-based ceramic electrolytes reason being their volume change giving rise to cracks on the surface upon cycling [28]. The sulfide-based electrolytes such as thio-LISICON or argyrodites, have the highest ionic conductivity of all, almost equivalent to liquid electrolytes but they tend to react with lithium metal enhancing the instability at the interface [29]. On the other hand, they are stable enough to counteract lithium dendrite formation and possess lower interfacial resistance. However, the commercialization of the solid-state batteries over liquid LIBs is still a challenge due to their insufficient contact between electrode/electrolyte interface and high processing temperature [30]. In comparison, the SPEs typically use polymers such as polyethylene oxide (PEO), poly(methyl methacrylate) (PMMA), poly (vinylidene fluoride-hexafluoropropylene) (PVDF-HFP), polyacrylonitrile (PAN) etc. specifically having polar groups to dissociate the lithium salts to generate more mobile Li^+ in the cell which thereby improves the lithium transference number [31–33]. Nonetheless, the SPEs alone suffer from low ionic conductivity and poor voltage endurance. Specifically, efforts have been made to enhance the ionic conductivity of the SPEs up to 10^{-3} S cm^{-1} or higher at room temperature by adding plasticizers, ionic liquids or solvents into the electrolytes which takes a toll on the stable electrolyte by compromising its mechanical strength and interface stability [34]. Such polymer electrolytes with liquid plasticizers or solvents added are known as gel polymer electrolytes (GPEs). Thus, CPEs build a bridge through the disparity between ISEs and SPEs. There are typically two variations of filler used being passive fillers and active fillers and they are also called solid plasticizers [35]. Inert fillers mainly consist of metal oxides like TiO_2, Al_2O_3, $BaTiO_3$, etc. or porous fillers which are MOF-based/carbon-based/clay-based fillers like graphene oxide, montmorillonite (MMT), etc. [36–40] These filler materials do not inherently possess mobile ion transport abilities but accelerates ion conduction by Lewis acid-base interactions and creating a pathway for free lithium ions to propagate through the polymer matrix [41]. In contrast, ISEs like $Li_7La_3Zr_2O_{12}$ (LLZO), $Li_{3x}La_{(2/3-x)}TiO_3$ (LLTO), $Li_{10}GeP_2S_{12}$ (LGPS), etc. are used as active fillers [42–44]. They introduce more free lithium ions in the system which creates steady ion channels or networks making the energy barrier of ion transportation low. Predominantly, in solid-state lithium-ion batteries $LiFePO_4$ has been shown to be a favourable cathode material due to its moderate working voltage (3.5 V vs. Li/Li^+), moderate capacity (170 mA h g^{-1}), flat voltage plateau, available material supply, low material cost, and acceptable environmental compatibility. The polymer electrolytes have an initial decomposition voltage of 3.9 V (vs Li/Li^+), and a phosphate cathode is more compatible with its low oxidation window. Thus, the flexibility and lower interfacial resistance of the SPEs and higher conductivity as well as mechanical strength to withstand lithium punctures are merged in one.

In this review, we focus on one particular polymer that is PVDF-HFP and explore into the work that has been done towards all solid-state lithium-ion battery (ASSB) and possibilities of future works as well. The PVDF-HFP is generally acquired by copolymerization of vinylidene difluoride (VDF) and hexafluoropropylene (HFP) [45]. It is well-known

as a copolymer of polyvinylidene difluoride (PVDF) which is incorporated with strong electron withdrawing group like (-CF_3) which enhances the extent of attracting the lithium ion from its anion in the salts and easily dissociates them due to its high dielectric constant ($\epsilon = 8.4$) [46]. The PVDF-HFP is composed of two phases: the crystalline phase serves as a mechanical support for the polymer electrolyte, while the amorphous component of the polymer aids in increased ionic conduction. Higher amorphicity would result from steric hindrance provided by the CF_3 pendant group in HFP monomers that are randomly mixed with VDF monomers. In addition, the PVDF-HFP contains fluorine having strong electricity absorption and cannot be readily oxidized by high-voltage cathodes, it can be employed as an electrolyte with high-voltage cathodes. Hence, these distinct properties make PVDF-HFP superior to rest of the polymers. The PVDF-HFP also demonstrates proper compatibility toward lithium metal, good miscibility for lithium salts and low glass transition temperature of −90 °C [47,48]. Therefore, the PVDF-HFP contains more amorphous domains which can effectively trap more lithium ions. Currently the sole SPEs made of the PVDF-HFP have an ionic conductivity in the range of 10^{-4} - 10^{-6} S cm^{-1} at room temperature which is quite low that can be increased drastically with the help of fillers [35,49]. Here, we aim to highlight all the CPEs established based on the PVDF-HFP as the polymer base with various fillers and discuss their fundamental interaction mechanisms including their performance in the cell and electrochemical stability during long cycling. Specifically, the contributions of the fillers on the anode and cathode electrolyte interfaces towards high conductivity, stability, high capacity, etc. are summed up. Finally, some future propositions for the development of CPEs for practical use in ASSB are reviewed.

2. PVDF-HFP polymer used as solid polymer electrolytes (SPE)

The primary requirement of the polymer used as electrolyte is its ability to dissociate the lithium salts into its counterparts i.e., the Li^+ ions and its corresponding anions. This dissociation of the salt gives rise to a greater number of mobile Li^+ leading to improvement in the ionic conduction. The presence of a greater number of polar groups like C═O, C–F, -N-, C═N, -*O*-, etc. in the polymers facilitates the desired process as reported by Zhou et al. [50–52] The dissociated lithium ions interact with the polar groups of the polymer and form polymer-salt complexes which establishes the segmental motion of the ion conduction in the polymers. The lithium ion hops from one coordination site formed by the polar groups in the chain of polymer to another coordination-site. This hopping mechanism and its dependence on the temperature can be explained by two predominant popular theories: the Arrhenius theory and the Vogel-Tamman-Fulcher (VTF) theory [53,54]. Materials which show linear variations in Arrhenius plots (σ vs 1/T) are indicative of straightforward hopping mechanism involved in the ion conduction whereas materials depicting non-linearity in the plot is suggestive of ion hopping along with contribution of segmental motion of the polymeric chains, both being coupled together [55]. However, ideally to ease and enhance the dissociation process of the salt, the polymer host should possess a certainly high dielectric constant whereas the salt should have lattice energy as low as possible to bring about the essential segmental motion in the polymer host further improving ion conductivity. It is generally seen that the ion conduction in the polymers take place only in the amorphous region and not the crystalline region. Here, the glass transition temperature of the polymer plays a major role below which the polymer becomes brittle and crystalline [56]. It is therefore preferred for the polymers to have glass transition temperature as low as possible so the working temperature range of the polymer is stretched wider.

The PVDF-HFP is widely attracting attention as a polymer that has lower degree of crystallinity as well as low glass transition temperature of −62 °C [57]. In addition, it has good thermal stability and also shows good solvent resistance with high polarity due to –CF_3 groups from the HFP monomer present in it. The higher amorphicity is due to the random combination of the VDF and the HFP monomers which introduce more irregularity among the polymer chains [58]. The acquired domains of the irregularities in the PVDF-HFP are otherwise crystalline in the PVDF making it semi-crystalline, providing less free volume for the ions, thus leading to poor conductivity [59]. It is believed that the crystalline part of the PVDF units cater to the mechanical strength of the matrix whereas the HFP units contribute towards the amorphicity [60]. The PVDF-HFP is hydrophobic due to the fluorine content of the HFP groups with a comparatively lower degree of crystallinity than the PVDF with high mechanical strength and flexibility, also having high polarity due to the presence of strong electron withdrawing groups [61,62]. Lithium salts are readily dissolvable in the PVDF-HFP matrix making it a strong candidate for the SPEs. The matrix has enhanced donor number for lithium ions due to the presence of the –CF and –CF_3 units which ascends the transport of ions from one chain to another either by intrachain or interchain segmental motion with breaking and forming of Li^+ bond to polar groups of the polymer matrix. Fig. 2 illustrates the lithium-ion conduction in the PVDF-HFP based CPEs. The ratio of the functional groups present in the polymer matrix to the lithium salts dissociated determines the ionic conductivity in the system. The molecular weight of the polymer matrix plays a vital role in long-range transport of the lithium ions through either of intrachain or interchain. This transfer is disrupted when molecular weight of the polymers is low, meaning the length of each polymer chain is not long enough for effective displacement of ions (segmental motions). The molecular weight of the PVDF-HFP is around 4,00,000 g mol^{-1} which makes it suitable for use in the solid polymer electrolytes [63].

Nevertheless, at room temperature finite the Li ion transport takes place and thus the ionic conductivity of the PVDF-HFP is restricted and does not meet the practical values during charging and discharging of the cells. However, finite Li ion transport is due to the higher degree of the crystallinity despite of the high dielectric constant ($\epsilon = 8.4$) of the matrix. To counteract this problem, crosslinking or blending of the polymers is done which slightly improves the ionic conductivity by forming more amorphous phase as ion conduction only appears in the amorphous regions of the PVDF-HFP. It is believed that the free volume in the polymer matrix increases where the diffusing ions can be situated by the above-mentioned means of blending of polymers, etc. and also the degree of crystallinity decreases slightly more that the PVDF-HFP matrix itself [64]. Thus, adjustment of the crystallinity plays the most vital role

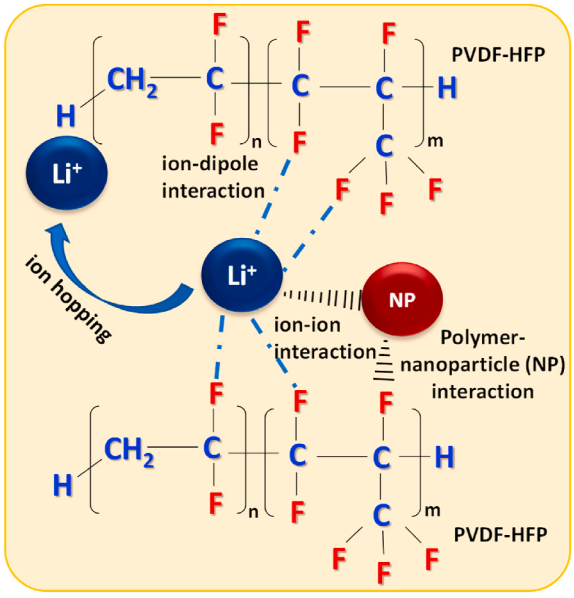

Fig. 2. Illustration of lithium ion conduction in PVDF-HFP polymer matrix in CPEs.

in ionic conductivity. Das et al., reported that the crystallinity of the polymers can be altered and adjusted by blending of polymers along with suitable percentage of plasticizer. They obtained an extremely amorphous phase at 30 % of ethylene carbonate (EC) along with a blend of PEO and the PVDF-HFP, and appropriate amount of $LiClO_4$ as the salt. Even, the ionic conductivity is seen to peak at 30 % of EC with 3.44×10^{-6} S cm^{-1} at room temperature [65]. Subramania et al., have obtained polymer blend films of PAN and the PVDF-HFP polymers via phase inversion method and reported an ionic conductivity as high as 3.41×10^{-3} S cm^{-1} at 25 °C [66]. At C/10 rate, the cell exhibited a discharge capacity of 135 mAh g^{-1}. Consequently, there is also an increase in transference number seen in the polymer blend as compared to the PAN or the PVDF-HFP alone. A polymer blended membrane of PVDF-HFP and PMMA with carboxymethyl cellulose (CMC) coating was studied by Guo et al. [67] It was observed that the introduction of surface coating could increase the ion migration by providing favourable wettability and enhance segmental movements of the polymer chains by reducing the crystallinity. The ionic conductivity could reach up to 4.388×10^{-3} S cm^{-1} at room temperature indicating the practical prospect of the blended polymers. The cell with CMC exhibited a higher initial discharge capacity of 162.5 mAh g^{-1} at 0.2 C-rate due to the enhanced Li^+ absorption rates. Therefore, the alteration of the degree of crystallinity and introduction of further amorphicity are researched on by plasticizing, copolymerization, blending of polymers, etc. [68] By impregnating electrolyte-affinitive poly(vinylidenefluoride-co-hexafluoropropylene) into ultra-light ~3 μm 3D-polytetrafluoroethylene scaffold, D. Chen et al. designed an ultraporous architecture to shorten Li^+ transfer pathways. Using $LiFePO_4$ as cathode, the electrolyte delivers a capacity of 118 mA h g^{-1} with an unmatched capacity retention of 90 % after 1000 cycles at 2C [69]. In spite of the above, due to the use of plasticizers there is a compromise on the mechanical strength of the polymer membrane which in turn do not suppress the lithium dendrite formation on the anode-electrolyte interphase. As a consequence, to improve the ionic conductivity at room temperature as well as the mechanical strength of the polymer electrolyte inhibiting punctures of lithium dendrites, various kinds of "fillers" also widely known as solid plasticizers are introduced into the system. These fillers also improve the overall electrochemical stability and are widely known as composite polymer electrolytes. They are viewed as a significant technique for boosting the PVDF-HFP-based polymer electrolytes in the future, as it can integrate the benefits of both the fillers and the polymer matrix.

3. PVDF-HFP polymer used as composite polymer electrolytes (CPEs)

It is observed that, in comparison to SPEs, CPEs have a much lower degree of crystallinity as well as better physical and electrochemical stability due to the lower glass transition temperature. In the presence of the fillers, the orderly arrangement of the crystalline regions of the polymer matrix is disrupted which enhances the ionic conductivity as the ion conduction takes place only in the amorphous spaces of the polymer electrolytes [70]. The decrease in the glass transition temperature is facilitated by the presence of the fillers as they extend the amorphization and aid in Li^+ ion movement in the polymer chains. They also play a role in prevention of stacking large spherulites one after another as they create a barrier that hinders the smooth movement of lithium ions [71]. Thus, the fillers inserted into the matrix reduce the size of spherulites and increase the amorphous phase and ease the lithium ions to diffuse by making a smooth pathway. Furthermore, the ion transport pathway created due to the fillers promotes swift transfer of lithium ions in the major portion of the composite electrolyte as well as the electrode/electrolyte interface thereby enhances the electrochemical performance due to decrease in the interfacial resistance. Primarily, the uniform dispersion of the inert fillers was widely researched on. In these kinds of materials, no active lithium ion was introduced into the electrolyte through the fillers where, metal oxides such as TiO_2, SiO_2, etc was incorporated and thus are called inert i.e., inert with respect to lithium ions [72,73]. Further, they contribute mainly in inhibiting the degree of crystallinity and in improving the movement ability of the PVDF-HFP segments. There are essentially four different kinds of inert fillers on the basis of what class of the materials they belong to for the fabrication of the PVDF-HFP made CPEs. They are namely ceramic (inert), ferroelectric ceramic, porous clusters, carbon-based materials or clays [74]. These fillers on their own do not have the ability to transfer lithium ions but they can create a more favourable environment for the hopping of Li^+ ions to take place. The physical and chemical interactions between the polymer and the filler are vital for achieving consequences like reduction in the degree of crystallinity and gaining more free volume in the bulk of the polymer, and also the effect of spherulites becoming smaller is a physical consequence. However, the chemical interaction involves the formation of Lewis acid-base interaction on the surface of the filler where lithium ion acts as the Lewis acid and interacts with the groups on the filler surfaces [75]. These interactions along with various other interactions like spontaneous polarization, osmotic behaviour, etc. thus increase the overall performance of the PVDF-HFP based polymer electrolytes.

3.1. Influence of various dimension fillers in PVDF-HFP based CPEs

The effect of size and morphology of the fillers on the ionic conduction principally stems from how it affects the ion transportation routes. Fig. 3 displays the structural representation of different fillers used in the PVDF-HFP based CPEs. Initially, researches focused on inorganic nanoparticle fillers without much concentration on the morphology which led to disconnected and short ion transfer routes. However, inorganic fillers possessing a high dimension aspect ratio can facilitate the formation of elongated and connected pathways for ion transfer, thus enhancing the Lithium-ion conductivity. So, with respect to morphology, fillers in the PVDF-HFP matrix can be classified into zero-dimensional (0D), one-dimensional (1D), two-dimensional (2D) and three-dimensional (3D) material structures as shown in Fig. 4.

The synthesis of 0D fillers is the easiest and the simplest, and various morphologies of such nanofillers can be achieved via different synthesis methods like sol-gel, hydrothermal, solution combustion, precipitation, etc. These synthesis routes are followed usually in the preparation of metal oxides or ferroelectric ceramic materials along with inorganic electrolyte active materials. The performance of the CPEs is exhibited based on the size or amount of the fillers used as well. If too much weight percentage of the filler was used with respect to the PVDF-HFP amount, that eventually led to agglomeration along with formation of more neutral ion pairs which do not allow the smooth transfer of lithium ions by blocking their transmission routes [77]. So, the right amount of the filler should be used to achieve the highest Li^+ ionic conductivity along with the expected mechanical strength improvement and decrease in the degree of the crystallinity. It is observed that for most cases at lower to moderate amount of the filler, the polymer-filler interaction is the most efficient. Tian et al. studied the influence of micro sized (Fig. 5(b)) and nano sized particles of niobium (V) oxide (Fig. 5(a)) in PVDF-HFP matrix and concluded that nanoparticles of Nb_2O_5 dispersed more uniformly in the polymer-salt mixture, and could be tape casted without agglomeration of the nanoparticles whereas, the micro particles of Nb_2O_5 showed a tendency towards agglomeration hindering the mobility of lithium ions [76]. Fig. 5(c and d) depicts the nano-CPE could cycle for over 200 h with a lower overpotential in comparison to the micro-CPE which underwent short circuiting after 80 h of cycling at current density 0.5 mA cm^{-2}.

1D fillers typically comprises of nanofibers or nanotubes morphology which are generated from 0D particles by being subjected to electrospinning after being dissolved in a solvent along with a highly conductive polymer [78]. They usually extend towards one direction in a continuous path which is beneficial for the ion migration as well. These

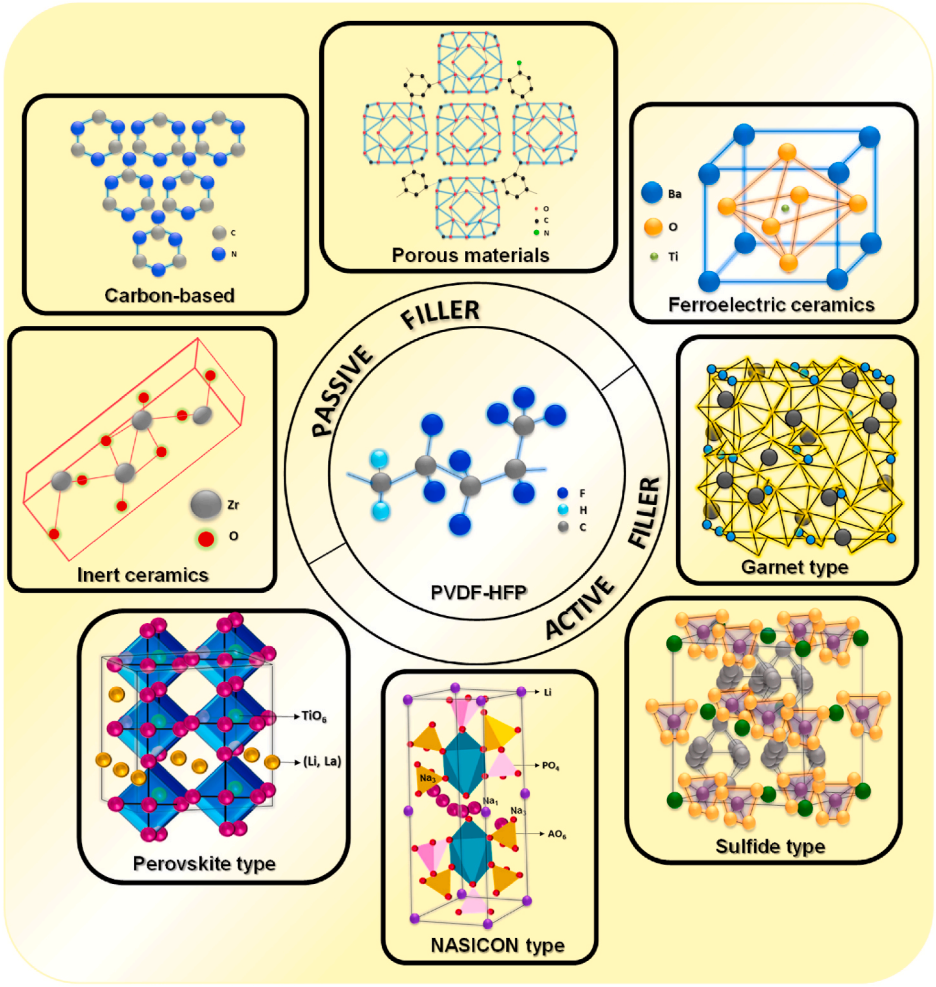

Fig. 3. Structural representation of various fillers used in PVDF-HFP based CPEs.

nanofibers or nanotubes can be classified on the basis of their orientation (random or aligned arrangements) as they have a major influence on the mechanism of the electrolyte. When the fillers possess a vertically aligned orientation, the lithium ion can transport with ease through the interfaces of the filler and the polymer matrix continuously which is also determined by the regularity of the active sites on the fillers whereas, when the orientation is random then, this pathway of ions through one nanotube for instance is hindered by another nanotube as they are distributed irregularly. Thus, linear arrangement of fillers can be advantageous in producing uninterrupted ion pathway across the bulk of the CPEs, leading to superior ionic conductivity. Wang et al., investigated the influence of homogeneously dispersed $Li_{6.25}Ga_{0.25}La_3Zr_2O_{12}$ (Ga-LLZO) nanofibers in PVDF-HFP matrix. It was observed that the CPE containing the Ga-LLZO nanofiber was electrochemically more stable as the crystallinity of the matrix was reduced and they provided continuous lithium-ion transport channels to rise up the ionic conductivity to 8.94 $\times 10^{-4}$ S cm^{-1} at 15 wt % [79]. The specific capacity of the full cell with $LiFePO_4$ (LFP) showed a specific capacity of 131 mAh g^{-1} at 0.1 C-rate along with 98.7 % coulombic efficiency (CE) and recovery capacity as the rate was decreased to 0.1 C-rate from 2 C-rate. Nevertheless, aligned arrangements of nanofibers have not been explored with PVDF-HFP polymer matrix as host. Liu et al. reported the effect of a vertically aligned $Li_{0.33}La_{0.557}TiO_3$ (LLTO) particles framework through ice templating method in PEO matrix in comparison to LLTO particles prepared from mechanical mixing [80]. It is observed that due to the change in orientation of the filler particles the ionic conductivity increases by 2.4 times suggesting that the uninterrupted vertical networks allow efficient transport of Li^+ ions. Further, to construct these uninterrupted conducting pathways even 2D sheet like (nanosheets) materials as fillers are explored in the PVDF-HFP host. Luo et al., prepared a 2D holey silica nanosheet (HSN) and incorporated it as filler in a PEO/PVDF-HFP blended polymer matrix. This filler could generate supplementary channels and decline the crystallinity thereby aiding ion conduction [81]. The presence of 2D-HSN exhibited a high Li^+ transference number of 0.34 as it enriched the ion migration environment and boosted ion transfer. The full cell with LFP as cathode delivered a high specific capacity of 159 mAh g^{-1} along with 95.5 % retention in capacity after 200 stable cycles.

In contrast to 1D or 2D materials, 3D material fillers have a more complicated structure comprising of various types like having highly porous surface or array like structures bundled together or a fully formed network-like structure. These 3D structures of the filler phase are generally acquired by adopting methods like hydrogel technology, high temperature annealing, etc. through which the lithium ions can penetrate and transport with ease. Thus, by applying a methodological approach towards the composition and structure of the filler, a robust and conducting interface can be attained. Yao et al., introduced nanoporous UiO-66 MOF in a PVDF-HFP polymer matrix which could expand the amorphous phases of the polymer and make the dissociation of the lithium salt more favourable along with the well-defined conductive channels located in, and along the filler itself can exhibit superior electrochemical performance of stable overpotential with no drastic polarization during 3500 h cycling at 0.2 mA cm^{-2}. Ionic conductivity of 1.1 mS cm^{-1} at 30 °C was attained due to enhanced movement of ions

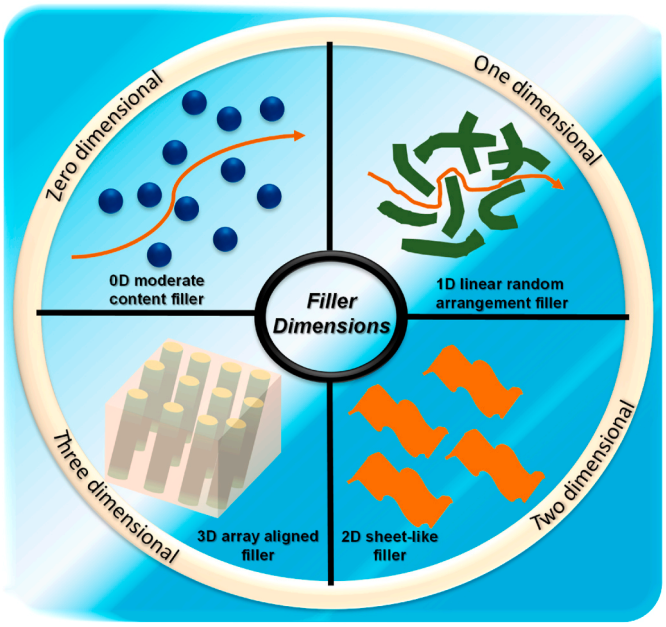

Fig. 4. Schematic illustration of various dimensional fillers used in PVDF-HFP based CPEs.

through the interfaces [82]. So, the mechanism through which ions are transporting through polymer matrices depends on the morphology, size and structure of the fillers used.

In summary, the range of fillers and composite techniques used in the PVDF-HFP-based CPEs results in a highly complex lithium-ion transport mechanism. This indicates that the composition approach with fillers and the architectures of the CPEs have a significant influence on the transport mechanism of lithium ions. Accordingly, rational composition and structural design can result in CPEs with strong ion conductivity and a stable interface, leading to stable and high discharge capacity.

3.2. Passive fillers used in PVDF-HFP matrix

3.2.1. Inert ceramic fillers with PVDF-HFP matrix

The incorporation of ceramic fillers into polymer matrix was first studied in the 1980's. Wieczorek et al., investigated the effect of ceramic alumina (Al_2O_3) particles on the flexible polymeric films in various weight proportions with respect to polymer as well as their grain sizes. Conductivity of about 10^{-5} S cm^{-1} was achieved at 30 °C at 10 wt% of 2 μm particle size of Al_2O_3. It was well established that the particle size played a major role in the diffusion of more mobile ions in 2 μm as compared to 4 μm particle size of Al_2O_3, the conductivity did not show any difference in comparison to the electrolyte without filler particles [83]. Similarly, various metal oxides and metal sulphides have been explored to elevate the ionic conductivity as well as add to the mechanical strength of the polymer electrolyte. They are predominantly in the particle size range of few micrometers or nanometers. Kumar et al., studied the upshot of using TiO_2 nanorods in place of submicron sized TiO_2 particles on the dispersion of filler and the porosity of the films. The ionic conductivity calculated using complex impedance measurements was found to be as high as 1.11×10^{-2} S cm^{-1} for the TiO_2 nanorods whereas for the submicron-sized TiO_2, the ionic conductivity was lower irrespective of the weight content of the filler used due to bigger particle size of the filler. Along with this, the rod-like morphology of crystalline TiO_2 enhanced the tensile strength up to 50 % [84]. Thus, the inclusion of the rod-shaped filler particles facilitated the smooth transfer of side chain dipoles within the PVDF-HFP polymer matrix. For a particular volume fraction, the tendency to diminish the interaction of the polymer host with the lithium metal is higher for micron-sized particles as they cover more area leading to obstruction in the passivation process. Agglomeration after a certain percentage of filler lead to the formation of an insulating layer at the interface causing increased impedance. On a whole, the properties of a superior CPE are not linearly dependent on one factor but can be controlled by variations in the filler type, size, structure, morphology as well as surface area i.e., porosity, weight

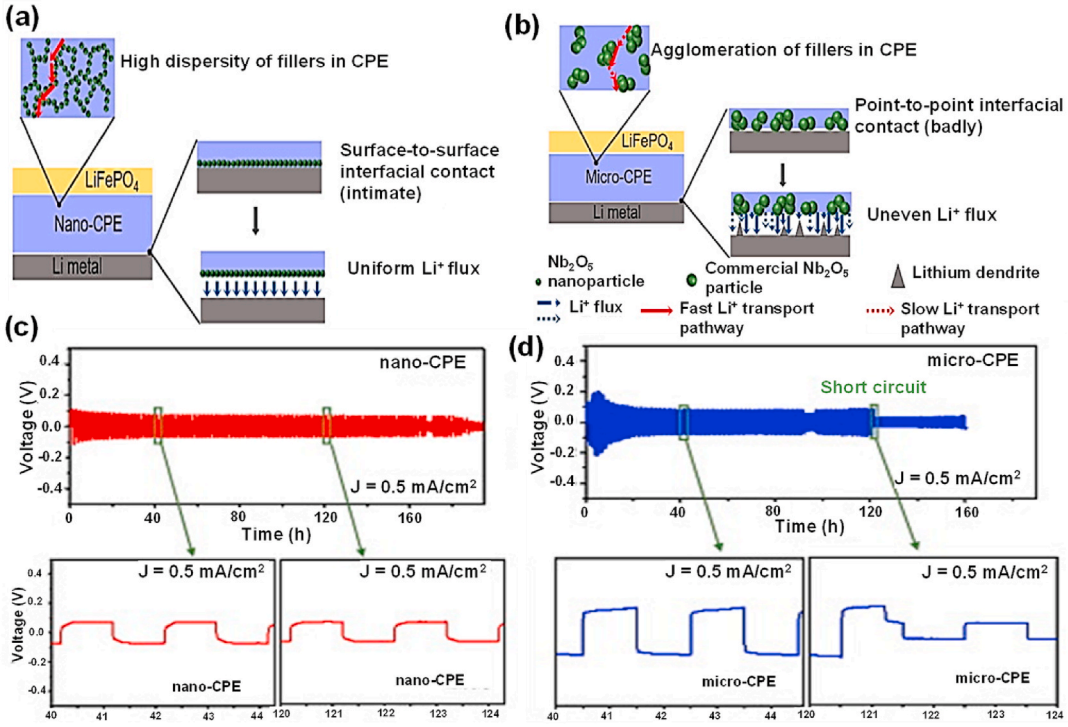

Fig. 5. Schematics of the mechanism of (a) nano-CPE, (b) micro CPE for Li^+ transportation and (c) Lithium stripping-plating profiles of SPE, nano and micro CPE at 0.5 mA cm^{-2}. Adapted with permission from ref. [76].

percentage, etc. The prime mechanism involved in this case is the formation of Lewis acid-base interactions between the filler surface and the anions of the salt [85]. The surface of the inert oxide fillers acts as Lewis acid and the counter anions of the lithium salts act as the corresponding Lewis base as they donate their electron pair. This interaction can be further accelerated and strengthened by introducing positively charged oxygen vacancies on the filler surface bringing about an enlarged release of mobile lithium ions which further amplifies the ionic conductivity. These mobile lithium ions will then be dispersed and transferred through hopping and segmental motions in the bulk of the polymer. The lone pairs of fluorine groups in the PVDF-HFP attract them and facilitate easy transport of ions, and increase the transference number of Li^+ of the CPE. Xiong et al., introduced oxygen vacancies boosted flower-like CeO_2 in PVDF-HFP matrix and found that the amplification of ionic conductivity up to 1.66×10^{-3} S cm^{-1} at room temperature as well as improved full cell discharge capacity as high as 166 mAh g^{-1} at 0.1C with a retention capacity of 83 mAh g^{-1} at 2 C-rate even at 1000 cycle is originated from the vacancies operating as Lewis-acid sites [86]. Furthermore, it was observed that oxygen vacancies lower the crystalline phase due to enriched predominant segmental movements in the amorphous phases. It is believed that oxygen vacancies can be intentionally introduced via doping. The fillers used can thus vary the dielectric properties of the composite polymer electrolytes. An interference of the fillers occurs in the regular arrangement of the polymer and salt i.e., -C-F$\cdots$$Li^+$ (ion-dipole interaction) in PVDF-HFP, impeding the mechanism between mutual polymer chains and causing the reduction in dielectric polarization. The surface modification of fillers to enhance the dispersibility also plays an important role. It was reported that with in-situ preparation methods for nanofillers, there was an improvement in the overall performance of the CPEs. The conventional way of preparing the nano-sized materials and adding it to the polymers sometimes lead to agglomerated condensed masses of fillers and obstructs the extent of amorphization of the CPE. Thus, in-situ synthesis of fillers via hydrolysis for PVDF-HFP matrix has been worked on. Cao et al., studied in-situ prepared nano-crystalline TiO_2–PMMA hybrid used as additive in PVDF-HFP and achieved an ionic conductivity as high as 2.77×10^{-3} S cm^{-1} at room temperature and thus it suggests that the PVDF-HFP matrix contains nanohybrids that are homogeneously distributed, resulting in favourable lithium-ion conduction paths around the particles and stronger interactions improving the conduction by suppressing the polymer crystallinity [87]. Additionally, the obtained discharge capacities at various current densities of the additive based CPE were significantly higher than that of the gel based electrolyte without nano-crystalline TiO_2–PMMA hybrid. Henceforth, lithium-ion transportation can take place in two ways i.e., primarily, the hopping of ions assisted by polar -C-F groups in PVDF-HFP and secondarily hopping assisted via the filler-polymer interfaces. So, the conduction mechanism of CPEs can be governed by the unique traits of variety of fillers.

3.2.2. Ferroelectric ceramic fillers with PVDF-HFP matrix

The benefits of using ceramic fillers having ferroelectric nature is that they can drastically increase the polarity of the electrolyte due to their intrinsic trait of having high dielectric constant which promotes effective charge separation contributing to increase in charge carriers. It also accelerates the salt dissociation process and produces lithium-ion with ease of formation which amplifies ionic conductivity of the CPEs for instance, $BaTiO_3$, $PbTiO_3$, $SrTiO_3$ etc. [88,89] The contribution towards better conductivity depends on the unique structures of ferroelectric materials that exhibit spontaneous polarization and their interaction with the lithium salts. This enhanced conductivity was well explained by interlinking the interaction between the lithium ions and the negative ions on the fillers surface and the precise trait of rapid polarization in ferroelectric ceramic materials. It is known that the grain size of the fillers compositing with polymers in their melt states generates poorly formed spherulites which result in increased amorphicity, ultimately increasing the ionic conductivity of the CPEs. Sasikumar et al., reported the formation of hydrothermally-derived nano-$BaTiO_3$ with cubic structure (Fig. 6(c–e)) as filler in PVDF-HFP/PVAc matrix and noted that the ionic conductivity ascended with increase in filler concentration and touched a maximum of 2.3×10^{-3} S cm^{-1} at 30 °C at 7.5 wt% with of the filler and then reduced with further increase of filler content as depicted in Fig. 6(d–f) [90]. This was due to the increase in the crystallinity after a certain extent of filler amount which aggravated the conduction paths to get blocked and thus decreased the ionic conductivity. The full cell performance also improved with the presence of the filler giving an initial discharge capacity of 132 mAh g^{-1} at 0.1C-rate and higher CE as compared to only SPE. Interestingly, Y. Ji et al., reported that ferroelectric ceramic $BaTiO_3$ can considerably prevent dendrite growth while keeping high mechanical strength when coupled with PVDF-HFP polymer to create a homogenous, single-layer composite separator with strong piezoelectric effects. The polarized composite polymer electrolyte in the Li|$LiFePO_4$ cell demonstrates a notably enhanced cycling performance, with over 99 % capacity retention after 400 cycles at 2C due to the piezoelectric mechanism [92]. However, the optimum amount of filler at which highest ionic conductivity achieved depends on the size as well as morphology of the filler incorporated and varies according to the filler grain size. The interaction of anions with lithium cations is rationalized by correlating the spontaneous polarization of ferroelectric ceramic materials leading to conductivity enhancement in the PVDF-HFP-Li-salt CPE. The effect of electric field ranging from 0 to 100 V cm^{-1} has been studied by Sunitha et al. using nano-ferroelectric ceramic materials on ionic conductivity in PEO polymer system [93]. It was observed that beyond electric field of 15 V cm^{-1} there was a notable increase of one order of magnitude in the ionic conductivity. With increase in the electric field, the lithium-ion activation barrier decreased exhibiting high values of ionic conductivity due to enhanced mobility of ions. Thus, similar studies involving electric field can be explored on PVDF-HFP based CPEs as well.

3.2.3. Porous materials fillers with PVDF-HFP matrix

The advantages of using porous materials as fillers in CPEs is that they provide numerous well-defined transmission pathways for lithium ions to propagate through their macromolecular porous structure acting as lithium hosts by creating profuse Lewis acid sites, and improving ion conduction and lithium ion transference. Specifically, a new class of materials known as metal-organic frameworks (MOFs) have captured huge attention as filler materials. They are macromolecular porous materials with metal ions in the center surrounded widely by organic ligands [94]. They can moderate the mechanical strength and inhibit the crystallinity as well as ionic conductivity when incorporated into PVDF-HFP polymer system. These organic linkers of the metal clusters have more affinity to interact with lithium ions and generate more Lewis acid-base pairs. Cui et al., incorporated ZIF-8 as a filler in PVDF-HFP matrix and achieved Li^+ transference number as high as 0.66 and ionic conductivity of 3.44×10^{-3} S cm^{-1} due to the nucleophilic effect and strong electronegativity of the imidazole group of ZIF-8 those reach out to bind with Li^+ via electrostatic attraction and thus facilitate swift transfer of ion through inner pathways [95]. The initial discharge capacity exhibited for the cell incorporated with ZIF-8 was 277.4 mAh g^{-1} being slightly higher that the SPE without filler being 264.9 mAh g^{-1} at 0.2C. Similarly, with the incorporation of UiO66 MOF filler, it was verified by DFT-MD simulations that it could enlarge the area of amorphous region in the PVDF-HFP polymer matrix by Yao et al. [82] The 4.5 wt% of filler exhibited an ionic conductivity of 1.1 mS cm^{-1} at 30 °C at 0.72 transference number for lithium. The full cell performance with respect to $LiFePO_4$ exhibited a capacity of 143.3 mAh g^{-1} at 10 C-rate after 300 cycles at 100 °C. Thus, the contribution of the MOFs on the ionic conductivity amplification depending on the loading content of the MOF filler in the electrolyte as well as the enhancement of porosity on the electrolyte surface is evident. Meanwhile, peripheral modification of MOFs can also be done using surface functionalized metal oxides that

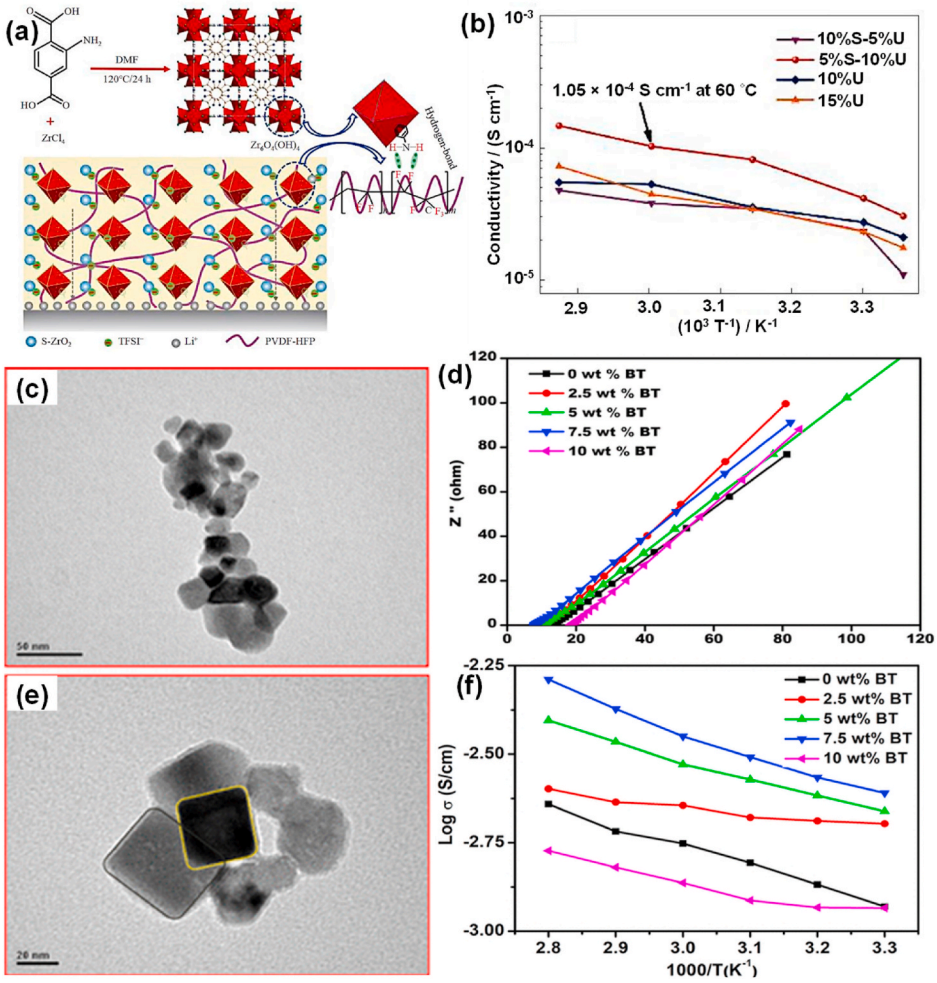

Fig. 6. (a) Arrhenius plots of the CPE with different ratios of the dual filler, (b) Schematic of dual filler superacid-ZrO_2 and UiO-66-NH_2 with PVDF-HFP,(c, e) TEM images of cubic-structured $BaTiO_3$, (d) Nyquist plots and (f) Arrhenius plots of cubic-structured $BaTiO_3$ at various weight percentages. Adapted with permission from ref. [90,91].

effectively induces anions in the medium to enhance the mobile lithium-ion migration rate. Wei et al., studied the performance of dual filler of nano-sized MOF UiO-66-NH_2 incorporated with superacid ZrO_2 [91]. Here, the strong immobilization of the ions take place due to presence of superacid via increased Lewis acid-base interactions on the interfaces leading to high lithium-ion transference number of 0.72. Structural stability is also reinforced by the contribution of hydrogen bonding interaction between the F atoms of PVDF-HFP matrix and $–NH_2$ groups of the MOFs displayed in Fig. 6(a). The nanosized MOF promoted the kinetics of ion migration by reducing the interfacial impedance and exhibiting an ionic conductivity of 1.05×10^{-4} S cm^{-1} at 60 °C (Fig. 6 (b)). The symmetric cell with the dual filler could stably operate beyond 600 h with short-circuiting at 0.05 mA cm^{-2} and an initial discharge capacity of 158 mAh g^{-1} at 0.2C-rate. Interestingly, MOFs along with ionic liquids like 1-ethyl-3-methylimidazolium bis[(trifluoromethyl)] sulfonyl]imide ($[EMIM]^+[TFSI]^-$) can trap anions in electrolyte through their nanopores without restricting the free flow of lithium ion in continuous channels due to their smaller radii as compared to the anions. Liu et al., reported a CPE demonstrating a homogeneous lithium-ion flux with ionic conductivity of 4.3×10^{-4} S cm^{-1} at room temperature with the above mechanism [96]. Microporous molecular sieves are a new type of materials which are used as fillers in CPEs due to their inherent properties like special pore size giving high surface area, highly selective nature and well-defined microstructures with ordered interconnected pathways [97]. Due to these properties, they are more superior to inert ceramic fillers as the porosity and the Lewis acid-base sites can be modulated which influences the lithium-ion transport and the ionic conductivity. Also, at the cation exchange centres in the interconnected channels of microporous molecular sieves, lithium ion can acquire the cation position during periodic replacement of anions in the framework and give rise to new pathways for lithium-ion conduction. Xiao et al., formed CPE by incorporating molecular sieve ZSM-5 which has mesoporous channel structure via steam bathing technique which showed significant enhancement in the electrochemical properties of the CPE as compared to vacuum drying and phase inversion methods. The ionic conductivity was enhanced by steam bathing to 5.1 mS cm^{-1} due to formation of well-uniform and aligned surface morphology accompanied by abundant interlinked pores on the layer of CPE also contributing to the vital interfacial properties [98]. The fabricated full cell with $LiCoO_2$ (LCO) exhibited a discharge capacity of 144.97 mAh g^{-1} at 0.1C-rate which was retained after cycling up to 97.5 % of its initial discharge capacity. As all molecular sieves vary in pore distribution as well as size in their ordered arrangements, they produce different surface morphology as well as electrochemical properties. Jiang et al., reported a comparative study of using three different molecular sieves namely NaY, MCM-41, and SBA-15 in PVDF-HFP to prepare microporous CPEs. SBA-15 based CPE that showed the best performance exhibiting rich pores on the surface leading to ionic conductivity of 0.50 mS cm^{-1} whereas NaY and MCM-41 showed compact structures with scarcely porous surface and reduced performance [99].

The full cell with SBA-15 was tested and it showed a coulombic efficiency of 87 % in the first cycle and also thereby retains its initial discharge capacity up to 94 % beyond 20 cycles. Thus, due to the presence of structured pores on the surface of MOFs can contribute towards the enhancement of lithium-ion transference number via various mechanisms mentioned above.

3.2.4. Carbon-based or clays with PVDF-HFP matrix

Clays have been seldom used as filler in polymer matrixes as they have distinct abilities of intercalation as they are multi-layered in structure with diverse morphologies along with their cation exchange capacity and ease of structural modification. The swelling processes upon addition of the clays facilitates the uniform dispersion of the fillers in the host polymer. The ability of nano-clays to intercalate can contribute in the appropriate functionalization of the layers to enhance the overall ion transfer kinetics. Out of several reported clay fillers in PVDF-HFP-based CPEs, montmorillonite (MMT) with special sandwich type structure is well explored by Solarajan et al., and could give ionic conductivity as high as 2.3×10^{-3} S cm^{-1} along with stable electrochemical window of 3.1 V [100]. Higher ion mobility in the polymer matrix intercalated within the MMT layers led to increased free volume effectively increasing ionic conductivity. Similarly, halloysite nanotube (HNT) clay having a 1D tube-like structure with superior mechanical features which restricted lithium dendrite formation and oppositely charged surfaces which majorly assists in the salt dissociation impacting the lithium-ion transference number. Zhang et al., reported the incorporation of the HNT filler in PVDF-HFP matrix and achieved an ionic conductivity of 1.23×10^{-3} S cm^{-1} at 6 wt percent filler with lithium ion transference number of 0.57, beyond which, agglomeration took place whereas for the electrolyte without filler exhibited a lower transference number of 0.43 [101]. The symmetric cell showed stability up to 800 h at 0.15 mA cm^{-2} current density and a 76 % capacity retention after 1000 cycles with respect to full cell fabricated with LFP. Thus, a very small amount directly influences the interfaces by the interaction of anionic parts of the salt with cationic aluminium hydroxyl groups located at the inner parts of HNTs with lithium-ion adsorption on the outer parts of HNTs amplifying the ion transference. Carbon-based materials are generally incorporated in electrode materials or used as frameworks for electrode to boost the conductivity. Here in polymer matrix, it has been proven to work as filler for better performing electrolyte with appropriately modifying the surface. The functionalization of 2D graphene has been explored for its ability to create more nucleation sites to prevent further growth of PVDF-HFP grains. The mechanical strength of the overall matrix is increased by the decrease in grain size by fine grain strengthening effect. The uniformly distributed anion groups throughout the 2D carbon layer also magnifies the segmental motion in the PVDF-HFP matrix at room temperature with consistent lithium-ion flux. Zhai et al., studied the influence of fluorinated graphene as filler in PVDF-HFP polymer and reported notable small grain size increased the transport of lithium-ion at the interface giving lithium-ion transference number of 0.472 as compared to polymer electrolyte without the filler of 0.315 [106]. From the Arrhenius plot derived from lithium-ion conductivities at various temperatures, it was seen that the activation energy was lower for the filler induced CPE and also the ratio of ion conductivity to electron conductivity was higher. This balance of conductivities could prevent the electronic conductivity of carbon from short circuiting the cell. The full cell with CPE and $LiNi_{0.6}Co_{0.2}Mn_{0.2}O_2$ (NCM622) as cathode exhibited a discharge capacity of 159.7 mAh g^{-1} at 0.2C-rate whereas the electrolyte without filler showed huge fluctuations in the capacity values at the same current rate. It is also observed as compared to one dimensional nanofillers that carbon functionalized nanosheets like g-C_3N_4 nanosheets can create an ion migration network with ease due to their large interface which potently amplifies the capacity of ion migration. Li et al., reported that the presence of g-C_3N_4 nanosheets in PVDF-HFP matrix effectively reduced the bulk impedance to 11.1 Ω with 15 wt% filler in the membrane which could be due to the sheet-like morphology and its surface enhanced with pyridine N working as a Lewis base which can accelerate the Li-ion transport by dissociating lithium salts [107]. The full cell with NCM622 exhibited a specific discharge capacity of 122.8 mAh g^{-1} at 0.5C-rate post 100 cycles.

Carbon-based materials like carbon nanotubes (CNTs) are often used as filler after certain targeted modifications. Xiao et al. studied reactions at the electrodes-electrolyte interface proceeded longer for electrolyte without modified-CNT filler as compared to with the filler which results in the increased resistance of electrolyte without the filler [108]. Thus, by further modifications of carbon-based fillers higher ionic conductivities can be achieved in the polymer electrolytes. As discussed here, Fig. 7 displays the various performance parameters of passive fillers in the form of bar diagram. In summary, with addition to slowing down the kinetics of crystallization, adding ceramic particles to SPEs can help the amorphous phase stay in place below room temperature. The increase in conductivity in CPEs can be ascribed to Lewis acid-base interactions or osmotic behaviour, and indirect specific interactions between the surface groups on filler particles and polymer chains and lithium salt anions. Furthermore, the addition of fillers to polymers does not dramatically alter the primary chain dynamics that drives ion transport. Instead of increasing the quantity of charge carriers, the addition of fillers to polymers merely results in an increase in the "free volume" and mobility of the polymer segment next to the filler surface. Therefore, the main variables influencing the ion conductivity of the CPEs are the content and dispersibility filler.

3.3. Active fillers used in PVDF-HFP matrix

3.3.1. Perovskite-type filler with PVDF-HFP matrix

As inert fillers can only decrease the lithium ions from impeding to a certain extent, it is necessary to introduce active fillers as they can more effectively, enhancing ionic conductivity by creating additional networks for lithium ion to transport. Generally, perovskite-type lithium lanthanum titanates (LLTO) are extensively used as fillers in CPEs due to its structural and chemical stabilities, facile preparation methods with ease of varying composition by doping, providing a wide and stable electrochemical window and show a bulk ionic conductivity as high as 10^{-3} S cm^{-1} [109]. Perovskites have a general formula of ABO_3 where A is occupied by a rare or alkaline earth metal ion and B is occupied by a transition metal ion. It is established that lithium ions propagate through the vacancies present in the A-site by a hopping mechanism. Thus, these vacancies can well be tuned by adjusting the composition of the metallic elements by methods like cation doping which is quite common. It has recently been studied that in the perovskites, the bulk ionic conductivity depends on the size of the doped A-site ion and also the strength of B–O bond [110–112]. So, A and B sites, both these centres have an impact on the ionic conductivity and can be substituted with different ionic-sized metals depending on their size, chemical reactivity, electronegativity, etc. Interestingly, anionic doping in LLTO particles also can modulate the ionic conductivity in CPEs due to differences in charge and ionicity of the metal-anion bonds. Yang et al., doped nitrogen in LLTO nanofibers (N-LLTO) where nitrogen with extra anionic charge could give rise to oxygen vacancies for charge balance. Additionally, difference in electronegativity of N (3.07) and O (3.50) resulted in a dissimilarity in the covalency of bonds thus exhibiting ionic conductivity of 3.8×10^{-4} S cm^{-1} at room temperature in PVDF-HFP polymer [113]. The symmetric cell fabricated with N-LLTO showed minimum polarization at same current densities as compared to pristine LLTO as filler which indicates the suppression of lithium dendrites. In CPEs, the effective lithium-ion transport of LLTO also depends on the nanoparticle surface, dimension, concentration and morphology. The transport of lithium ions primarily occurs through host PVDF-HFP phase itself, the active LLTO filler only provides a secondary ion transfer network which does not overpower the primary mode of lithium transfer. Cation doping is also quite often done with Al^{3+}, nevertheless, it is studied that A-LLTO is

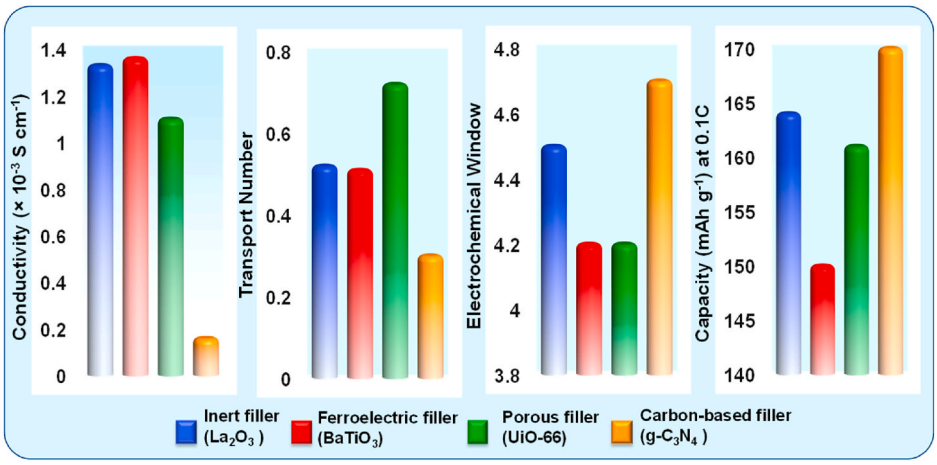

Fig. 7. Bar diagram representation of various parameters in different kinds of passive fillers. Adapted with permission from ref. [102–105].

somewhat chemically unstable when in contact with Li metal. Thus, to overcome this problem, ultrathin coating or encapsulation of the A-LLTO particles was carried out. Le et al., modified the surface of A-LLTO using SiO_2 (Fig. 8(d)) which is stable against lithium metal and the thickness of coating is maintained very thin enough to not hinder ion transportation [114]. The adhesion between polymer and salts on the exterior surface of the coated SiO_2 also increases. Notably, the coating of SiO_2 (Fig. 8(e)) lead to a slight decrease in the ionic conductivity in the CPE due to its electrical resistant nature but was still comparable to other reported CPEs. Galvanostatic cycling of the symmetric cell showed a very low and stable overpotential up to 1922 h at 0.48 mA cm^{-2}. Post 500 cycles the full cell with LCO retained initial capacity to 80.5 % and coulombic efficiency as high as 99.2 % whereas the discharge capacity of SPE without filler declined significantly. Furthermore, Zhu et al., could achieve an ionic conductivity up to 2.18 × 10^{-4} S cm^{-1} at room temperature and electrochemically stable window up to 4.8 V with LLTO nanorods of diameter 200 nm synthesized through electrospinning [115]. These LLTO nanorods could significantly disrupt the ordered PVDF-HFP host and boost the lithium-ion shuttling efficiently. The Li/Li symmetric cell could run stably for over 2000 h at current density of 0.1 mA cm^{-2}. The fabricated full cell with NCM622 as cathode showed a discharge capacity of 142 mAh g^{-1} with 84.6 % retention rate after long cycling. Thus, the nanorod-like morphology of the LLTO filler played a crucial role in creating increased ion transport paths. Additionally, the influence of alignment of nanorods or nanowires is another factor that has been widely explored in CPEs and it is seen that highly aligned networks get ten times higher ionic conductivity as compared to randomly oriented nanowires. Further studies on the morphology of perovskite fillers in PVDF-HFP matrix and its effect on the performance of CPEs could be the focus of upcoming research.

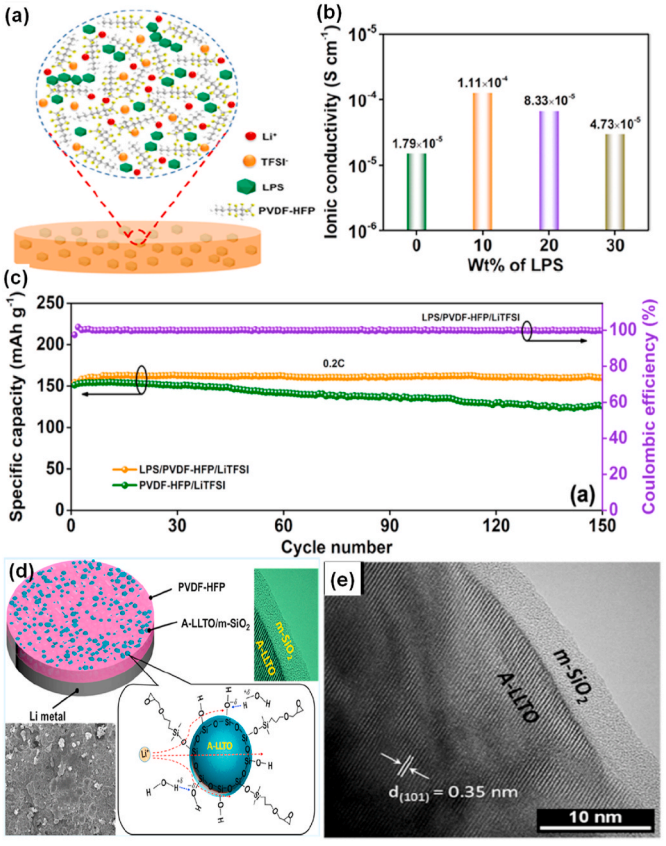

Fig. 8. (a) Schematic illustrations of CPE with LPS filler, (b) Comparison of ionic conductivities at various ratios of LPS filler, (c) LFP||Li cycling performance at 0.2C and coulombic efficiency, (d) Schematic of Al-LLTO encapsulation with SiO_2 and (e) TEM image of the A-LLTO/m-SiO_2 particles. Adapted with permission from ref. [114,116].

3.3.2. *Garnet-type filler with PVDF-HFP matrix*

Garnet-type $Li_7La_3Zr_2O_{12}$ (LLZO) solid electrolytes are the most promising type of active fillers due to its high compatibility with lithium metal giving wide electrochemical stability window and high bulk ionic conductivity of 10^{-3} S cm^{-1} at room temperature [117]. They primarily exists in two stable phases i.e., the tetragonal and cubic phase out of which, ionic conductivity is high for the cubic phase although the tetragonal phase can be easily stabilized at low temperature [118]. With high temperature sintering, the stable cubic phase is achieved which exhibits high ionic conductivity and is utilized as filler in CPEs. Li et al., reported the role of 10 wt % LLZO 1D-structured nanofibers in PVDF-HFP polymer host which exhibited an improved ionic conductivity of 9.5 × 10^{-4} S cm^{-1} at room temperature [119]. The interaction between LLZO and PVDF-HFP led to more flexibility in local chains along with the contribution of rich vacancies on the surface of the cubic LLZO nanofibers which boosted the lithium ion hopping mechanism as they could hop by replacing consecutive vacancy positions. The full cell with LFP as cathode manifested a discharge capacity of 140 mAh g^{-1} and coulombic efficiency of 99.9 % upon cycling. However, doping garnet-type materials with different aliovalent cations like Al^{3+}, Ta^{4+}, etc. for LLZO cubic phase stabilization is also preferred. Beshahwured et al., synthesized cubic phase ligament-like morphology of aluminium-doped LLZO (A-LLZO) using double-template method and incorporated 12 wt % as filler in PVDF-HFP to attain an ionic

conductivity of 1.12 × 10^{-4} S cm^{-1} which is still lower than Li et al., since the 1D structure allows the creation of more Li-pathways [120]. Here, the full cell with A-LLZO CPE exhibited a specific discharge capacity of 160.92 mAh g^{-1} at 0.1C-rate with a retention capacity of 92.52 % after cycling. Similarly, tantalum-doped LLZO showed an ionic conductivity in the same range of 10^{-3} - 10^{-4} S cm^{-1}. Zhang et al., reported the variation in ionic conductivity with respect to the size of the filler. It was observed that the nanosized LLZTO (N-LLZTO) particles in the PEO polymer showed almost 100 times greater ionic conductivity in comparison with micron-sized particles as fillers [121]. Thus, on the basis of size and larger surface area in nano-sized LLZTO particles, Xu et al., comprehensively increased the performance by incorporating it as filler in PVDF-HFP polymer matrix as shown in Fig. 9(a–d). Here, N-LLZTO partially activates dehydrofluorination of the PVDF-HFP matrix that enhances Li^+ coordination thereby leading to rapid dissociation of lithium salt and form 3D conduction pathways exhibiting an ionic conduction of 1.7 × 10^{-4} S cm^{-1} at room temperature (Fig. 9(e and f)) [122]. The CPE at 20 wt % filler showed a stable electrochemical window up to 4.8 V with lithium-ion transference number as high as 0.57. The full cell $LiFePO_4$/Li batteries showed a discharge capacity of 136.6 mAh g^{-1} at 0.5C-rate along with initial capacity retention of 94.6 %. However, the ionic conductivity of the LLZO is restricted to ~10^{-4} S cm^{-1} due to less surface area of the particles synthesized through conventional methods which shortens the ion-conduction pathways. Tao et al., designed a method of using MOFs as template due to their high surface area and extreme porous nature to synthesize cubic phase LLZO. These special structured fillers allow the creation of more ion migration channels as they also have porous channel-like structure inherently. The CPE exhibited an ionic conductivity of 5.47 × 10^{-4} S cm^{-1} at 60 °C with an electrochemically stable window of 4.85 V [123]. The assembled

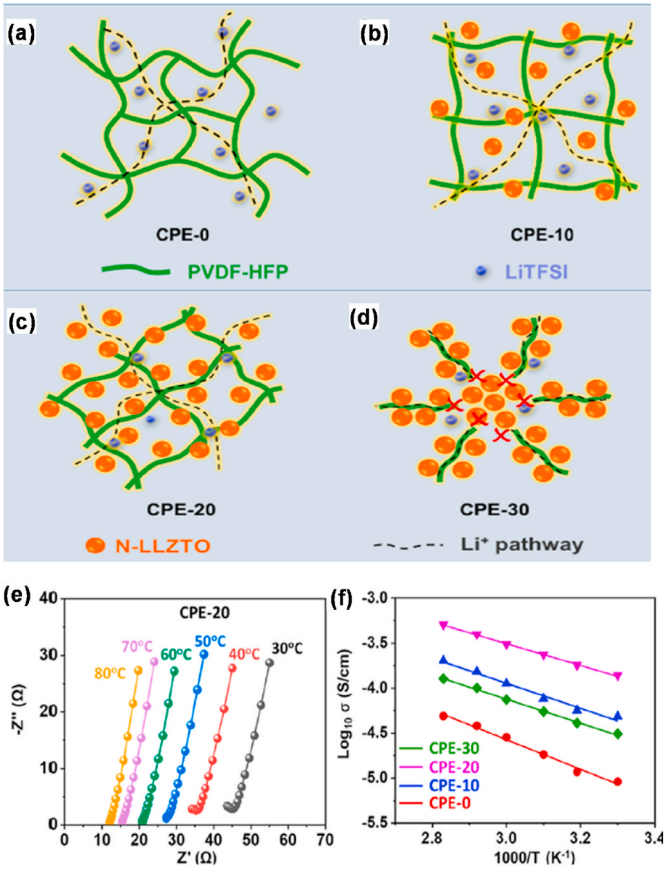

Fig. 9. (a–d) Schematic illustrations of different weight percentage of fillers, (e) Nyquist plots and (f) Arrhenius plots for CPE with 20 wt percent filler in PVDF-HFP. Adapted with permission from ref. [122].

$LiFePO_4$/Li full cell manifested an initial discharge capacity of 135 mAh g^{-1} at 0.5C-rate with capacity retention of 83.51 % post 500 cycles. Similarly, Sun et al., introduced different sizes (micron and nano sized) of Cu-(1,3,5-benzenetricarboxylicacid)-1 (HKUST-1) MOF in the PVDF-HFP polymer along with $Li_{6.75}La_3Zr_{1.75}Nb_{0.25}O_{12}$ (LLZN) garnet-typed nanowire fillers [124]. It is reported that the micron sized MOFs provide more mechanical strength to the CPE inhibiting lithium dendrites from forming and the nanosized MOFs could offset gaps between particles to create more continuous flow of lithium ions [125]. The coarse surfaced LLZN nanowires contributed in lowering the activation energy along the interface with its large aspect ratio. The CPE exhibited an ionic conductivity of 2 × 10^{-4} S cm^{-1} in ambient atmosphere and the Li/Li symmetric cell could cycle stably for 1700 h at 0.25 mA cm^{-2}. Thus, the CPEs fabricated with garnet-type particles as filler show good electrochemical stability and also comparable ionic conductivities. In general, adding garnet-type particles to the PVDF-HFP can considerably increase the interfacial stability between CPEs and the lithium anode, making it particularly suitable as fillers.

3.3.3. *Sulfide-type filler with PVDF-HFP matrix*

Sulfides as electrolytes have the highest ionic conductivity and exhibit low grain boundary resistance as compared to the oxide-based inorganic solid electrolytes but unfortunately are the least explored type due to their instability towards air and moisture [126]. Consequently, the sulfide-based electrolytes are barely possible to store in moisture as they react to produce harmful gases like H_2S that led to degradation of the electrolyte which restricts the scale-up. It is also reported that polar solvents used for CPEs like N-methyl-2-pyrrolidinone (NMP), acetone, etc. amplifies the degradation and dissolution of the electrolyte. Thus, it is crucial to choose a suitable solvent as well. Another issue with the sulfide electrolytes is their very narrow stable electrochemical window of 1.7–2.1 V. Majorly, the sulfide solid-state electrolytes are divided into two types, thio-LISICON $Li_{4-x}Ge_{1-x}P_xS_4$ ($0<x<1$) (LGPS) and argyrodites Li_6PS_5X (X = Cl, Br, I). Once these electrolytes come in contact with lithium metal, they establish new reduced interphases with low ionic conductivity such as (Li_2S, Li_3P and $Li_{15}Ge_4$), increasing the impedance at the metal/electrolyte interphase [127]. Nevertheless, inspite of these issues, as the sulfides have the highest ionic conductivity efforts were being made towards designing novel compositions with the use of appropriate solvent. Li et al., demonstrated a novel CPEs that exhibited good air stability and enhanced electrochemical stability as PVDF-HFP could protect Li_7PS_6 (LPS) from the hydrolysis reaction when exposed to moisture [116]. Hence, LPS interacts effectively by acting as cross-linking sites in the polymer increasing the amorphous phases (Fig. 8(a)). After optimization, at 10 wt% of LPS, the highest ionic conductivity of 1.11 × 10^{-4} S cm^{-1} was achieved as shown in Fig. 8(b). Additionally, the electrochemical compatibility with lithium when evaluated using stripping/-plating studies showed stable cycling of 2000 h at 0.2 mA cm^{-2} as compared to the polymer electrolyte without filler. The Li/LFP full cell exhibited a specific capacity of 160 mAh g^{-1} at 0.2C-rate beyond 150 cycles as shown in Fig. 8(c). Further, Cong et al., tactifully employed mono-alcohol perfluoropolyethers as co-solvents and dimethyl carbonate terminated perfluoropolyethers as interfacial stabilizers against lithium metal which manifested stable potential window until 4.8 V [128]. This electrochemical stability is attributed to the lowering of HOMO and LUMO levels by fluorine substitution in the solvent causing increased oxidation stability. According to this film making procedure an ionic conductivity of 0.18 mS cm^{-1} and a high transport number of 0.68 were achieved. The symmetric cell could cycle beyond 1200 at 0.1 mA cm^{-2} and the full cell coupled with LFP displayed specific capacity of 158 mAh g^{-1} at 0.05C-rate. Further inspired from the sulfide electrolytes having high ionic conductivity and advantageous lamellar structure materials, Tao et al., fabricated a novel $3Li_2S$–$2MoS_2$ (LMS), active intercalated filler combining both with immense lithium ion transport channels via ball-milling followed by quenching [129]. The

long chains of PVDF-HFP gets slackened due to the incorporation of LMS enhancing the ion mobility. The lewis acid sites of PVDF-HFP also weakened the salt anions association and accelerated the dissociation as the LMS acted as a physical plasticizer. Thus the prepared LMS at 12 wt % presented an ionic conductivity of 1.17 × 10^{-4} S cm^{-1} at room temperature with a wide electrochemical stability window up to 4.8 V. The constructed Li/$LiCoO_2$ cell delivered a discharge capacity of 145.79 mAh g^{-1} at 0.5C along with capacity retention of more than 86.22 %.

3.3.4. NASICON-type filler with PVDF-HFP matrix

The most widely explored NASICON-type inorganic solid electrolytes are lithium aluminium titanium phosphate $Li_{(1+x)}Al_xTi_{(2-x)}(PO_4)_3$, (LATP) and lithium aluminium germanium phosphate $Li_{(1+x)}Al_xGe_{(2-x)}(PO_4)_3$ (LAGP). They are considered promising due to their great stability in air and fast ionic conductivity (10^{-4} - 10^{-3} S cm^{-1}) [130–132]. However, to attain reduced grain boundary and proper phase formation and fast ionic conductivity, NASICON-type electrolytes require elevated temperatures and prolonged time for densification which is difficult to scale up. Due to the brittle nature of the NASICON-type inorganic solid electrolytes, they are favoured to be used as fillers in CPEs which gives a new perspective of flexibility mechanical properties along with increased ionic conductivity in the PVDF-HFP matrix. There are various methods of synthesizing NASICON-type fillers like sol-gel method, solid-phase method, melt-quenching method, etc. ultimately reflecting in their particle size and morphology [133–135]. Andreev et al., studied the influence of particle size on the ionic transport of LATP prepared from sol-gel method in comparison with solid-phase method in PVDF-HFP [136]. The LATP prepared by solid-phase method revealed an average particle size of 5 μm as compared to uniformly sized 0.3 μm by sol-gel method. Consequently, it was observed that the conductivity activation energy was lower for the sol-gel method-formed LATP. The conductivity increase with concentration also depends on the particle size of the filler. Smaller particle fillers tend to agglomerate more than larger particle size fillers so the amount of the filler added should be systematically adjusted and optimized. Li et al., synthesized LATP via sol-gel method assisted with citric acid which was embedded smoothly on the PVDF-HFP matrix and had microporous surface which exhibited an ionic conductivity of 2.3 × 10^{-4} S cm^{-1} at 10 wt% with no added electrolyte uptake and good cyclability [137]. The full cell comprised of LFP as cathode demonstrated an initial specific capacity of 150 mAh g^{-1} and retained up to 130 mAh g^{-1} post 50 cycles at 0.2C-rate. Further, to regulate the interfacial distribution of ionic charge carriers, 2D nanomaterial like graphitic carbon nitride (g-CN) with inherent polarity and high surface area is introduced along with LATP in PVDF-HFP by Zhang et al. Additionally, here the g-CN disrupts the ordered folding of PVDF-HFP decreasing the crystallization and improving the ionic conductivity of the CPE to 2.11 × 10^{-4} S cm^{-1} at 80 °C as compared to the CPE with solely LATP exhibiting ionic conductivity of 1.68 × 10^{-4} S cm^{-1} at 80 °C [142]. Moreover, surface modification by functionalization of LATP with groups like silane could enhance the Lewis acid sites by fully exposing them which further increase anion absorption ability thereby maximizing the ion transfer ability. Table 1 shows the performance of various fillers and their reported parameters with respect to weight percentages of filler used for PVDF-HFP based CPEs. It is also noted that all kinds of active fillers work differently and vary performance-wise as summarised in Fig. 10 in the form of bar diagram.

In conclusion, ion conduction materials have more successful roles as active fillers to enhance the performance of the CPEs because inert fillers can provide only decrease in crystallinity and improve in mechanical support to the CPE. Solid-state electrolytes with a high number of ion transference and high inherent room temperature conductivity are commonly found in garnet-type $Li_7La_3Zr_2O_{12}$, $Li_{10}GeP_2S_{12}$, etc. Large grain boundary resistance and poor electrode/electrolyte interfacial stability are two drawbacks that still restrict the use of solid-state electrolytes as active fillers in the CPEs. To create an efficient composite, the benefits of the polymer and inorganic solid-state electrolytes must be combined while accounting for mechanical and ion transport characteristics.

3.4. Interface at the PVDF-HFP based CPE and the electrode

The interfacial stability and resistance are the most challenging issues to overcome in all solid-state batteries. Polymer-based electrolytes have better interfacial contact as compared to ceramic electrolytes as they are more flexible. However, it is necessary to achieve ionic conductivity and interfacial wettability in the range of liquid electrolytes for the solid electrolytes to be fully developed for practical use. Research has been focused mainly on improving the solid-solid contact features leading to effects on ionic conductivity. Interfacial contact determines the overall parameters of a battery like cyclability, ion transfer number, ion conductivity, chemical as well as electrochemical stability. The interfacial impedance also largely determines the power output of the cell and the frequency of lithium ions present in the bulk. The mechanical strength at the CPE interfaces determines the amount of

Table 1
Performance of various passive and active fillers at respective temperatures reported for PVDF-HFP based CPEs.

Type of filler	Electrolyte composition	Ionic conductivity (S cm^{-1})	Temperature (°C)	Ref.
Passive fillers				
TiO_2 nanorods	PVDF-HFP/$LiClO_4$/5 % TiO_2	1.72 × 10^{-4}	RT	[145]
Nano-$BaTiO_3$ (BT)	PVDF-HFP/PVAc/LiTFSI/7.5% BT	2.0 × 10^{-3}	RT	[146]
Spherical zirconium dioxide (ZrO_2)	PVDF-HFP/PMMA/LiTFSI/6% ZrO_2	1.46 × 10^{-3}	25	[147]
Single-layer layered-double-hydroxide nanosheets (SLN)	PVDF-HFP/LiTFSI/1 % SLN	2.2 × 10^{-4}	25	[148]
MOF-5	PVDF-HFP/LiTFSI/2 % MOF-5	1.20 × 10^{-3}	RT	[149]
Covalent linked 2,2''-(ethylenedioxy) bis (ethylamine) to reduced graphene oxide (rGO-PEG-NH_2)	PVDF-HFP/LiTFSI/10 % rGO-PEG-NH_2	2.1 × 10^{-3}	30	[150]
2D Boron nitride (BN)	PVDF-HFP/LiTFSI/1 % BN	1.82 × 10^{-3}	RT	[151]
Al_2O_3 particles	PVDF-HFP/LiTFSI/2 % Al_2O_3	5.26 × 10^{-3}	25	[152]
Active fillers				
$Li_{0.33}La_{0.557}TiO_3$ (LLTO) nanorods	PVDF-HFP/LiTFSI/10%LLTO	2.18 × 10^{-4}	RT	[153]
$Li_{1.5}Al_{0.5}Ge_{1.5}P_{2.9}Si_{0.1}O1_2$ (LAGP) glass	PVDF-HFP/LiTFSI/20%LAGP	4.49 × 10^{-3}	RT	[154]
$Li_{6.25}Al_{0.25}La_3Zr_2O_{12}$ (Al-LLZO)	PVDF-HFP/LiTFSI/12%Al-LLZO	0.28 × 10^{-3}	RT	[155]
Nitrogen doped-$Li_{3x}La_{2/3-x}TiO_3$ (N-LLTO) nanofibers	PVDF-HFP/LiTFSI/30%N-LLTO	3.8 × 10^{-4}	RT	[156]
$Na_{1.3+x}Al_{0.3}Ce_xTi_{1.7-x}(PO_4)_3$ (NCATP)	PVDF-HFP/LiTFSI/30%NCATP	2.16 × 10^{-3}	25	[157]
$Li_{6.5}La_3Zr_{1.5}Ta_{0.5}O_{12}$ (LLZTO)	PVDF-HFP/LiTFSI/12.5%LLZTO	1.61 × 10^{-3}	80	[158]
$3Li_2S–2MoS_2$ (LMS)	PVDF-HFP/LiODFB/12%LMS	1.17 × 10^{-4}	30	[159]
$Li_7La_3Zr_2O_{12}$ (LLZO) nanofiber	PVDF-HFP/LiTFSI/10%LLZO	9.5 × 10^{-4}	RT	[160]
Li_7PS_6 (LPS)	PVDF-HFP/LiTFSI/10%LPS	1.1 × 10^{-4}	RT	[161]

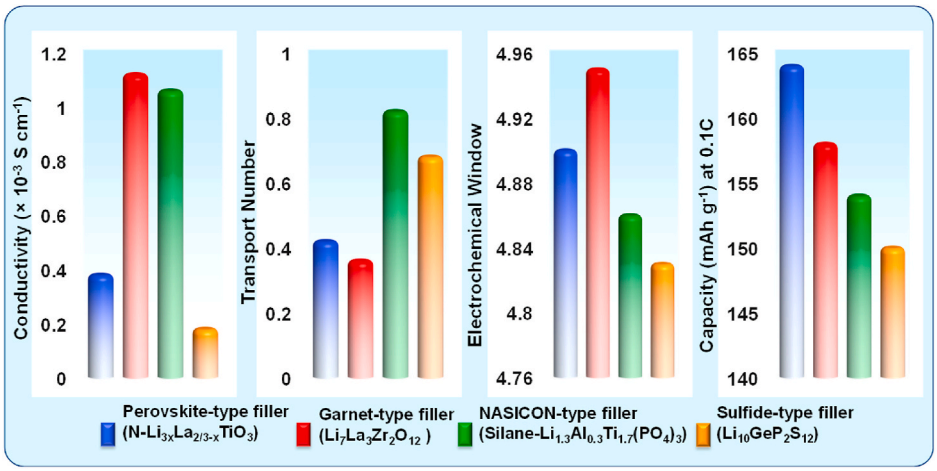

Fig. 10. Bar diagram representation of various parameters in different kinds of active fillers. Adapted with permission from ref. [138–141].

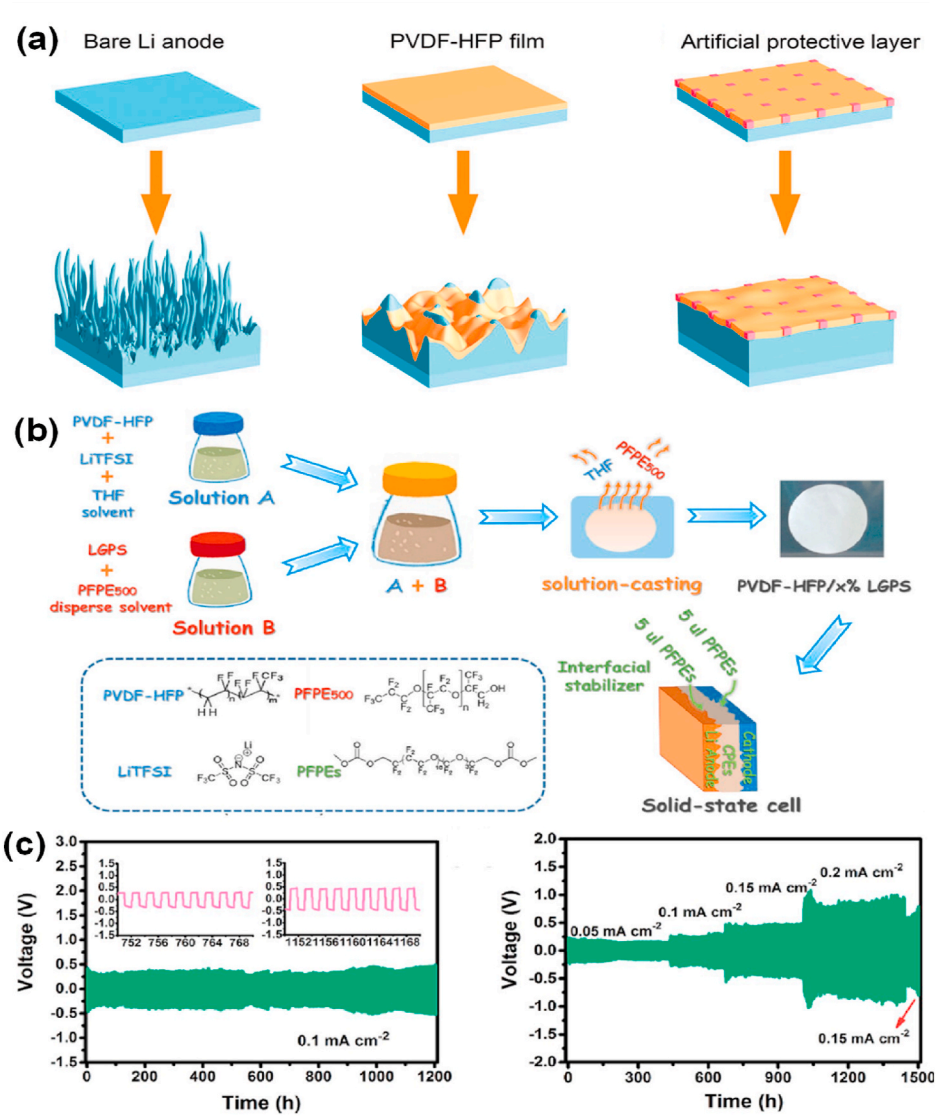

Fig. 11. (a) Schematic illustration of Li deposition on bare Li anode, PVDF-HFP film and artificial protective layer (b) Schematic of the preparation procedure of PVDF-HFP/PFPEs/x wt. % LGPS (x = 10, 20 and 30) CPEs and (c) Lithium stripping-plating profiles at various current densities with PVDF-HFP/PFPEs/LGPS CPE. Adapted with permission from ref. [143,144].

dendrite formation that can be suppressed on long cycling. Electrode deformation and electrochemical instability are mainly due to the unwanted reactions that take place at the interfaces. Here, various ways to improve the interfacial contact are discussed with respect to lithium metal anode as well as cathodes with the PVDF-HFP based CPE. The most crucial challenge on the lithium anode side is the lithium dendrite growth as the CPE do not have the mechanical strength to withstand them on cycling thereby, lowering the coulombic efficiency. Thus, this factor is majorly hindering the use of lithium metal as anode in batteries. It is noteworthy that solid electrolytes were once considered as a remedy to lithium dendrites formed in presence of liquid electrolytes but it is proven that ISEs and CPEs still exhibit major dendrite formation. Further for SPEs, the mechanical strength is compromised even more as they perform effectively at higher temperatures whereas in CPEs the addition of fillers reinforces the mechanical strength to an extent. It is also necessary to develop a clear mechanism of lithium dendrites at the interface between a solid electrolyte and a lithium anode to achieve the homogeneous deposition of dendritic-free lithium at the interface. Thus, to overcome this uncontrollable growth of dendrites and highly unstable interface, an artificial protective layer (APL) is often casted on the lithium metal anode as shown in Fig. 11(a). The APL is composed of inorganic lithium fluoride and organic PVDF-HFP, rationally hybridized into a film on the lithium metal anode. The various advantages of the formed APL were reflected in the coulombic efficiency (>99.2 %) of the full cell with $LiFePO_4$ as cathode. The improved performance was attributed to the features of the APL like good stability with lithium metal, increased mechanical modulus and optimized dendrite-free deposition of lithium during long cycle range. Along with incorporation of LiF particles, the APL has mesoporous morphology with pore size 2.5–12 nm with bimodal distribution. These pores can conduct rapid lithium-ion diffusion but cannot accommodate micro-sized Li dendrites. The LiF particles also increases the Young's modulus largely (6.72 GPa) as compared to the pristine PVDF-HFP film (0.8 GPa), preventing the growth of dendrites [143]. Another way to reduce interfacial resistance is the addition of few drops of liquid electrolyte as wetting agent to promote the ion transfer kinetics. A restricted amount of liquid electrolyte does not compromise the safety of the battery largely whereas it instantly makes the cell performance better. Interfacial stabilizers also dramatically improve the stability at the interfaces and cell performance. Cong et al., incorporated few drops of high molecular weight perfluoropolyethers (PFPEs) which forms a stable electrolyte interface in-situ that is rich in LiF (Fig. 11(b)) [144]. Here, the lithium stripping/plating studies in the cell with interface stabilizer PFPEs showed a stable and flat profile beyond 1200 h at 0.1 mA cm^{-2} (Fig. 11(c)). As for the cathode and CPE interface, PVDF-HFP polymer has a low oxidation window and decomposition voltage around 4 V so they are most compatible with low voltage cathodes like $LiFePO_4$. The construction of composite cathode is quite explored where the cathode active material is uniformly dispersed in a solvent along with the composite polymer electrolyte slurry and cast on Al foil to form an intimate interfacial contact between the cathode and the CPE. This improves the wettability at the interface drastically enhancing the adhesion at the interface. Du et al., reported a composite cathode with LFP and PVDF-HFP polymer in DMF solvent which exhibited an excellent interfacial compatibility as the symmetric cell could be continuously cycled for over 1000 h at 0.1 mA cm^{-2} with very low overpotential [162]. Thus, composite cathode method does solve the interfacial issues largely but it simultaneously reduces the proportion of active material due to which the battery capacity and energy density is compromised. One of the most important approaches for getting high energy density all-solid-state lithium batteries is a high-voltage composite cathode. The interface stability of the cathode and the PVDF-HFP-based CPE must be carefully taken into account and regulated. High electrochemical/chemical stability, dependable flexibility and soft contact with the cathode, and strong antioxidation ability at high voltage are the qualities that the cathode-modified layer should display. The anode-modified layer must have the following characteristics of strong chemical and electrochemical stability, efficient dendritic growth suppression, good mechanical robustness and flexibility and good anti-reduction ability at low voltage. These factors thus hinder the development of all solid-state batteries effectively. Thus, optimization and stabilization of the electrolyte/electrode interfaces in all solid-state batteries are the main focus for future research. Another new method involves in-situ polymerization of a polymer at the solid-solid contacts to develop adhesion. Ma et al., optimized the interface at the cathode and PVDF-HFP-LiTFSI membrane via in-situ polymerization of poly (ethylene glycol) diacrylate which tightly binds them both leading to huge decrease in interfacial impedance from 9380 Ω cm^2 to 1100 Ω cm^2 [163]. This is an advanced method as compared to the traditional method of adding few drops of liquid electrolyte for improving the interfacial wetting. To achieve higher energy density solid-state batteries, we need to focus on incorporating high voltage cathode which is not possible without improving the interfacial stability as PVDF-HFP based CPE will lead to degradation. H K Tran et al., prepared a sandwich like composite polymer electrolyte with Al-LLZO as filler in the main layer along with PVDF-HFP and polypropylene carbonate (PPC) blend polymer and sandwiched it with skin layers with the same just excluding the filler [164]. The presence of these skin layers on either side could enhance interfacial contact and make the electrolyte compatible with high voltage Al_2O_3–C@NCA ($LiNi_{1-x-y}Co_xAl_yO_2$) cathode with a wide electrochemically stable window of 4.9 V. Thus, all solid-state batteries aim to achieve high energy density as well as stability at the electrolyte-electrode interface which is the current concern for the research community at present. Looking out for new methods to modify the interfaces is one promising approach towards development of better performing all solid-state batteries. An outline on the future directions of PVDF-HFP based CPE is shown in Fig. 12. Thus, in order to build high-performance all-solid-state lithium batteries, the interface between a CPE and an electrode is crucial, particularly for the interfacial stability of the high-voltage cathode side and the development of lithium dendrites on the lithium anode side. To enhance the compatibility of CPEs with the low-voltage cathode and the interfacial stability of the high-voltage cathode, the cathode side typically employs the strategies of a composite cathode and cathode surface modification. However, it is highly difficult for a basic CPE to stop the growth of lithium dendrites on the lithium anode side; as a result, creating an artificial SEI layer becomes a practical technical approach for altering the anode/CPE interface.

4. Conclusion

In summary, we reviewed PVDF-HFP based CPEs for next generation all solid-state lithium-ion batteries as they have the salient features of both ISEs and SPEs with high-safety and energy. As several polymers are

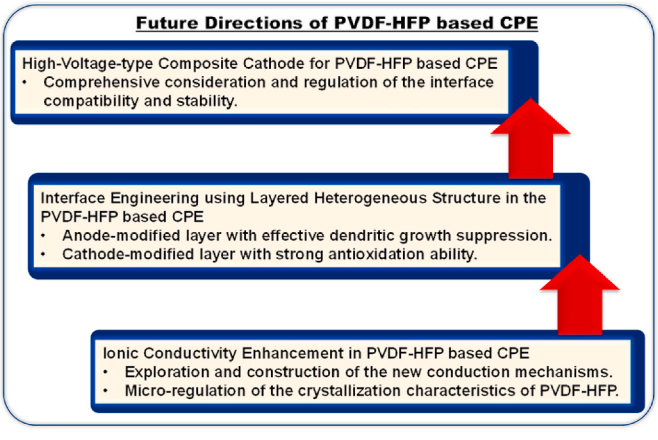

Fig. 12. Schematic of the future directions of PVDF-HFP CPE.

utilized for developing CPEs, on a deeper macroscopic or microscopic level they all differ. The inherent features of the polymer determine the structure, degree of crystallinity and aggregation of a polymer on a macro level. Here, PVDF-HFP has been focused on as at its macro level, its low glass transition temperature enhances the degree of amorphous phase which favours ionic conduction of Li^+. The lithium salt dissociation ability is also highly favoured due to its high dielectric constant. On a microscopic level, the structural changes and ion conduction pathways in a polymer are well controlled by the incorporation of fillers as PVDF-HFP by itself is restricted by its low mechanical strength and ionic conductivity. It is required to use appropriate amount of fillers to hinder aggregation or segmental motion in polymer for conduction. The fillers dictate the ion transport pathway as has been discussed with Lewis-acid base interaction (passive fillers) between salt, filler and polymer or by introducing lithium ions in the system by themselves (active fillers). It is noteworthy that the amount of active filler used in CPEs are always higher in comparison to passive fillers until the aggregation of fillers take place. Various dimension and structures of fillers like spherical nanoparticles, nanorods, 3D frameworks, etc. also largely influence in construction of the ion conduction routes as has been discussed. In recent times, improvements of bulk ionic conductivities and stable electrochemical window with prolonged cycle life using several fillers have come a long way. The establishment of new mechanisms of conduction need new materials to be explored with several additives for improved performance. As we know transport of lithium ions rely on the interfacial contact so, further, the electrode-electrolyte interface studies should be focused on in the future to avoid dendrite formation on the anode interface and achieve more electrochemical stability on the cathode interface. The capability of the cathode interface to withstand higher voltage is a crucial dictator in producing high energy density batteries. Thus, these bottlenecks should be dug into for achieving the promising high energy density batteries for commercial use.

Dedication

Dedication PE dedicates this article to Prof. N. Munichandraiah, Professor Emeritus, Indian Institute of Science Bangalore on his 72nd Birth Day

CRediT authorship contribution statement

Bhargabi Halder: Writing – original draft, Writing – review & editing. **Mohamed Gamal Mohamed:** Writing – review & editing. **Shiao-Wei Kuo:** Writing – review & editing. **Perumal Elumalai:** Supervision, Writing – review & editing.

Declaration of competing interest

The authors declare that they have no known competing financial interests or personal relationships that could have appeared to influence the work reported in this paper.

Data availability

Data will be made available on request.

Acknowledgements

PE thanks the Science and Engineering Research Board (SERB), Government of India, under the research grant (CRG/2021/005678) and Central Power Research Institute, Bangalore (CPRI) under the research grant (CPRI/R&D/TC/GDEC/2023). BH thanks CSIR-UGC for the Junior Research Fellowship (E-81088). MGM and SWK thank the Ministry of Science and Technology, Taiwan, under contracts NSTC 110-2124-M-002-013 and 111-2223-E-110-004 for the financial support.

References

[1] T. Ahmad, D. Zhang, A critical review of comparative global historical energy consumption and future demand: the story told so far, Energy Rep. 6 (2020) 1973–1991, https://doi.org/10.1016/j.egyr.2020.07.020.
[2] J.J. Siirola, Speculations on global energy demand and supply going forward, Curr Opin Chem Eng 5 (2014) 96–100, https://doi.org/10.1016/j.coche.2014.07.002.
[3] J. Skea, R. van Diemen, J. Portugal-Pereira, A Al Khourdajie, Outlooks, explorations and normative scenarios: approaches to global energy futures compared, Technol. Forecast. Soc. Change 168 (2021) 120736, https://doi.org/10.1016/j.techfore.2021.120736.
[4] P.J. Hall, E.J. Bain, Energy-storage technologies and electricity generation, Energy Pol. 36 (2008) 4352–4355, https://doi.org/10.1016/j.enpol.2008.09.037.
[5] J.H. Kim, Grand challenges and opportunities in batteries and electrochemistry, Frontiers in Batteries and Electrochemistry 1 (2022), https://doi.org/10.3389/fbael.2022.1066276.
[6] E.M. Erickson, C. Ghanty, D. Aurbach, New horizons for conventional lithium-ion battery technology, J. Phys. Chem. Lett. 5 (2014) 3313–3324, https://doi.org/10.1021/jz501387m.
[7] T. Maiyalagan, P. Elumalai. Rechargeable Lithium-Ion Batteries: Trends and Progress in Electric Vehicles, CRC Press, 2020. https://doi.org/10.1201/9781351052702.
[8] B. Scrosati, J. Hassoun, Y.-K. Sun, Lithium-ion batteries. A look into the future, Energy Environ. Sci. 4 (2011) 3287, https://doi.org/10.1039/c1ee01388b.
[9] X. Tian, Y. Yi, B. Fang, et al., Design strategies of safe electrolytes for preventing thermal runaway in lithium-ion batteries, Chem. Mater. 32 (2020) 9821–9848, https://doi.org/10.1021/acs.chemmater.0c02428.
[10] M.H. Braga, N.S. Grundish, A.J. Murchison, J.B. Goodenough, Alternative strategy for a safe rechargeable battery, Energy Environ. Sci. 10 (2017) 331–336, https://doi.org/10.1039/C6EE02888H.
[11] R. Chen, Q. Li, X. Yu, et al., Approaching practically accessible solid-state batteries: stability issues related to solid electrolytes and interfaces, Chem. Rev. 120 (2020) 6820–6877.
[12] H. Yang, J. Li, Z. Sun, et al., Reliable liquid electrolytes for lithium metal batteries, Energy Storage Mater. 30 (2020) 113–129, https://doi.org/10.1016/j.ensm.2020.04.010.
[13] S. Rahardian, B.A. Budiman, P. Lebdo Sambegoro, I.P. Nurprasetio, Review of solid-state battery technology progress, in: 2019 6th International Conference on Electric Vehicular Technology (ICEVT), IEEE, 2019, pp. 310–315.
[14] S. Lou, F. Zhang, C. Fu, et al., Interface issues and challenges in all-solid-state batteries: lithium, sodium, and beyond, Adv. Mater. 33 (2021) 2000721, https://doi.org/10.1002/adma.202000721.
[15] E. Kartini, C. Theresa Genardy, The future of all solid state battery, IOP Conf. Ser. Mater. Sci. Eng. 924 (2020) 012038, https://doi.org/10.1088/1757-899X/924/1/012038.
[16] Q. Yu, K. Jiang, C. Yu, et al., Recent progress of composite solid polymer electrolytes for all-solid-state lithium metal batteries, Chin. Chem. Lett. 32 (2021) 2659–2678, https://doi.org/10.1016/j.cclet.2021.03.032.
[17] F. Lv, Z. Wang, L. Shi, et al., Challenges and development of composite solid-state electrolytes for high-performance lithium-ion batteries, J. Power Sources 441 (2019) 227175, https://doi.org/10.1016/j.jpowsour.2019.227175.
[18] M. Dirican, C. Yan, P. Zhu, X. Zhang, Composite solid electrolytes for all-solid-state lithium batteries, Mater. Sci. Eng. R Rep. 136 (2019) 27–46, https://doi.org/10.1016/j.mser.2018.10.004.
[19] J.R. Nair, F. Bella, N. Angulakshmi, et al., Nanocellulose-laden composite polymer electrolytes for high performing lithium–sulphur batteries, Energy Storage Mater. 3 (2016) 69–76, https://doi.org/10.1016/j.ensm.2016.01.008.
[20] K. Zhang, S. Mu, W. Liu, et al., A flexible NASICON-type composite electrolyte for lithium-oxygen/air battery, Ionics 25 (2019) 25–33, https://doi.org/10.1007/s11581-018-2580-9.
[21] M.S. Park, S.B. Ma, D.J. Lee, et al., A highly reversible lithium metal anode, Sci. Rep. 4 (2014) 3815, https://doi.org/10.1038/srep03815.
[22] X. Guan, Y. Zhao, H. Pei, et al., Metalloporphyrin conjugated porous polymer in-situ grown on a Celgard separator as multifunctional polysulfide barrier and catalyst for high-performance Li-S batteries, Chem. Eng. J. 473 (2023) 144733, https://doi.org/10.1016/j.cej.2023.144733.
[23] J. Janek, W.G. Zeier, A solid future for battery development, Nat. Energy 1 (2016) 16141, https://doi.org/10.1038/nenergy.2016.141.
[24] H.J. Choi, S.Y. Kim, M.K. Gong, et al., Tailored perovskite $Li_{0.33}La_{0.56}TiO_3$ via an adipic acid-assisted solution process: a promising solid electrolyte for lithium batteries, J. Alloys Compd. 729 (2017) 338–343, https://doi.org/10.1016/j.jallcom.2017.09.160.
[25] G.V. Alexander, O.V. Sreejith, M.S. Indu, R. Murugan, Interface-compatible and high-cyclability lithiophilic lithium–zinc alloy anodes for garnet-structured solid electrolytes, ACS Appl. Energy Mater. 3 (2020) 9010–9017, https://doi.org/10.1021/acsaem.0c01430.
[26] A. Paolella, X. Liu, A. Daali, et al., Enabling high-performance NASICON-based solid-state lithium metal batteries towards practical conditions, Adv. Funct. Mater. 31 (2021), https://doi.org/10.1002/adfm.202102765.
[27] F. Han, Y. Zhu, X. He, et al., Electrochemical stability of $Li_{10}GeP_2S_{12}$ and $Li_7La_3Zr_2O_{12}$ solid electrolytes, Adv. Energy Mater. 6 (2016) 1501590, https://doi.org/10.1002/aenm.201501590.
[28] K.J. Kim, M. Balaish, M. Wadaguchi, et al., Solid-state Li–metal batteries: challenges and horizons of oxide and sulfide solid electrolytes and their

interfaces, Adv. Energy Mater. 11 (2021) 2002689, https://doi.org/10.1002/aenm.202002689.
[29] D. Liu, W. Zhu, Z. Feng, et al., Recent progress in sulfide-based solid electrolytes for Li-ion batteries, Mater. Sci. Eng., B 213 (2016) 169–176, https://doi.org/10.1016/j.mseb.2016.03.005.
[30] A. Mauger, M. Armand, C.M. Julien, K. Zaghib, Challenges and issues facing lithium metal for solid-state rechargeable batteries, J. Power Sources 353 (2017) 333–342, https://doi.org/10.1016/j.jpowsour.2017.04.018.
[31] Q. Zhang, K. Liu, F. Ding, X. Liu, Recent advances in solid polymer electrolytes for lithium batteries, Nano Res. 10 (2017) 4139–4174, https://doi.org/10.1007/s12274-017-1763-4.
[32] M.G. Mohamed, S.V. Chaganti, S.U. Sharma, et al., Constructing conjugated microporous polymers containing the pyrene-4,5,9,10-tetraone unit for energy storage, ACS Appl. Energy Mater. 5 (2022) 10130–10140, https://doi.org/10.1021/acsaem.2c01842.
[33] T.-H. Weng, M.G. Mohamed, S.U. Sharma, et al., Ultrastable three-dimensional triptycene- and tetraphenylethene-conjugated microporous polymers for energy storage, ACS Appl. Energy Mater. 5 (2022) 14239–14249, https://doi.org/10.1021/acsaem.2c02809.
[34] J. Shin, Ionic liquids to the rescue? Overcoming the ionic conductivity limitations of polymer electrolytes, Electrochem. Commun. 5 (2003) 1016–1020, https://doi.org/10.1016/j.elecom.2003.09.017.
[35] X. Yang, J. Liu, N. Pei, et al., The critical role of fillers in composite polymer electrolytes for lithium battery, Nano-Micro Lett. 15 (2023).
[36] J. Cao, L. Wang, Y. Shang, et al., Dispersibility of nano-TiO_2 on performance of composite polymer electrolytes for Li-ion batteries, Electrochim. Acta 111 (2013) 674–679, https://doi.org/10.1016/j.electacta.2013.08.048.
[37] L. Wang, J. Yan, R. Zhang, et al., Core–Shell PMIA@PVdF-HFP/Al2O3 nanofiber mats in situ coaxial electrospun on LiFePO4 electrode as matrices for gel electrolytes, ACS Appl. Mater. Interfaces 13 (2021) 9875–9884, https://doi.org/10.1021/acsami.0c20854.
[38] P. Prabakaran, R.P. Manimuthu, S. Gurusamy, Influence of barium titanate nanofiller on PEO/PVdF-HFP blend-based polymer electrolyte membrane for Li-battery applications, J. Solid State Electrochem. 21 (2017) 1273–1285, https://doi.org/10.1007/s10008-016-3477-z.
[39] S. Pavithra, A. Sakunthala, S. Rajesh, et al., Influence of graphene oxide on the membrane characteristics of PVDF-HFP as an electrolyte for lithium-based energy storage devices, Appl. Nanosci. 13 (2023) 4177–4192, https://doi.org/10.1007/s13204-023-02839-w.
[40] M. Wang, F. Zhao, Z. Guo, S. Dong, Poly(vinylidene fluoride-hexafluoropropylene)/organo-montmorillonite clays nanocomposite lithium polymer electrolytes, Electrochim. Acta 49 (2004) 3595–3602, https://doi.org/10.1016/j.electacta.2004.03.028.
[41] A. Manuel Stephan, K.S. Nahm, T. Prem Kumar, et al., Nanofiller incorporated poly(vinylidene fluoride–hexafluoropropylene) (PVdF–HFP) composite electrolytes for lithium batteries, J. Power Sources 159 (2006) 1316–1321, https://doi.org/10.1016/j.jpowsour.2005.11.055.
[42] W. He, H. Ding, X. Chen, W. Yang, Three-dimensional LLZO/PVDF-HFP fiber network-enhanced ultrathin composite solid electrolyte membrane for dendrite-free solid-state lithium metal batteries, J. Membr. Sci. 665 (2023) 121095, https://doi.org/10.1016/j.memsci.2022.121095.
[43] Q. Zhang, F. Ding, W. Sun, L. Sang, Preparation of LAGP/P(VDF-HFP) polymer electrolytes for Li-ion batteries, RSC Adv. 5 (2015) 65395–65401, https://doi.org/10.1039/C5RA09837H.
[44] X. Zhao, C. Wang, H. Liu, et al., A review of polymer-based solid-state electrolytes for lithium-metal batteries: structure, kinetic, interface stability, and application, Batter Supercaps 6 (2023), https://doi.org/10.1002/batt.202200502.
[45] W. Xiao, X. Li, H. Guo, et al., Preparation of core–shell structural single ionic conductor SiO_2@Li+ and its application in PVDF–HFP-based composite polymer electrolyte, Electrochim. Acta 85 (2012) 612–621, https://doi.org/10.1016/j.electacta.2012.08.120.
[46] W. Han, T. Kim, B. Yoo, H.-H. Park, Tunable dielectric properties of poly (vinylidenefluoride-co-hexafluoropropylene) films with embedded fluorinated barium strontium titanate nanoparticles, Sci. Rep. 8 (2018) 4086, https://doi.org/10.1038/s41598-018-22442-2.
[47] X. Liu, J. Liu, B. Lin, et al., PVDF-HFP-Based composite electrolyte membranes having high conductivity and lithium-ion transference number for lithium metal batteries, ACS Appl. Energy Mater. 5 (2022) 1031–1040, https://doi.org/10.1021/acsaem.1c03417.
[48] H. Xie, Z. Tang, Z. Li, et al., PVDF-HFP composite polymer electrolyte with excellent electrochemical properties for Li-ion batteries, J. Solid State Electrochem. 12 (2008) 1497–1502, https://doi.org/10.1007/s10008-008-0511-9.
[49] A. Manuel Stephan, Review on gel polymer electrolytes for lithium batteries, Eur. Polym. J. 42 (2006) 21–42, https://doi.org/10.1016/j.eurpolymj.2005.09.017.
[50] A. Arya, A.L. Sharma, Polymer electrolytes for lithium-ion batteries: a critical study, Ionics 23 (2017) 497–540, https://doi.org/10.1007/s11581-016-1908-6.
[51] Q. Zhou, J. Ma, S. Dong, et al., Intermolecular chemistry in solid polymer electrolytes for high-energy-density lithium batteries, Adv. Mater. 31 (2019) 1902029, https://doi.org/10.1002/adma.201902029.
[52] M.G. Mohamed, S.U. Sharma, C.-H. Yang, et al., Anthraquinone-enriched conjugated microporous polymers as organic cathode materials for high-performance lithium-ion batteries, ACS Appl. Energy Mater. 4 (2021) 14628–14639, https://doi.org/10.1021/acsaem.1c03270.
[53] S.B. Aziz, T.J. Woo, M.F.Z. Kadir, H.M. Ahmed, A conceptual review on polymer electrolytes and ion transport models, J. Sci.: Advanced Materials and Devices 3 (2018) 1–17, https://doi.org/10.1016/j.jsamd.2018.01.002.
[54] G. Girish Kumar, N. Munichandraiah, Solid-state rechargeable magnesium cell with poly(vinylidenefluoride)–magnesium triflate gel polymer electrolyte, J. Power Sources 102 (2001) 46–54, https://doi.org/10.1016/S0378-7753(01)00772-8.
[55] S.D. Druger, Ionic transport in polymer electrolytes based on renewing environments, J. Chem. Phys. 100 (1994) 3979–3984, https://doi.org/10.1063/1.466331.
[56] B.K. Money, K. Hariharan, J. Swenson, Glass transition and relaxation processes of nanocomposite polymer electrolytes, J. Phys. Chem. B 116 (2012) 7762–7770, https://doi.org/10.1021/jp3036499.
[57] H. Xie, Z. Tang, Z. Li, et al., PVDF-HFP composite polymer electrolyte with excellent electrochemical properties for Li-ion batteries, J. Solid State Electrochem. 12 (2008) 1497–1502, https://doi.org/10.1007/s10008-008-0511-9.
[58] N. Ataollahi, A. Ahmad, H. Hamzah, et al., Preparation and characterization of PVDF-HFP/MG49 based polymer blend electrolyte, Int. J. Electrochem. Sci. 7 (2012) 6693–6703, https://doi.org/10.1016/S1452-3981(23)15740-3.
[59] S. Abbrent, J. Plestil, D. Hlavata, et al., Crystallinity and morphology of PVdF–HFP-based gel electrolytes, Polymer (Guildf) 42 (2001) 1407–1416, https://doi.org/10.1016/S0032-3861(00)00517-6.
[60] M.A. Gebreyesus, Y. Purushotham, J.S. Kumar, Preparation and characterization of lithium ion conducting polymer electrolytes based on a blend of poly (vinylidene fluoride-co-hexafluoropropylene) and poly(methyl methacrylate), Heliyon 2 (2016), https://doi.org/10.1016/j.heliyon.2016.e00134.
[61] D. Saikia, H.Y. Wu, Y.C. Pan, et al., Highly conductive and electrochemically stable plasticized blend polymer electrolytes based on PVdF-HFP and triblock copolymer PPG-PEG-PPG diamine for Li-ion batteries, J. Power Sources 196 (2011) 2826–2834, https://doi.org/10.1016/j.jpowsour.2010.10.096.
[62] S. Wongchitphimon, R. Wang, R. Jiraratananon, et al., Effect of polyethylene glycol (PEG) as an additive on the fabrication of polyvinylidene fluoride-co-hexafluropropylene (PVDF-HFP) asymmetric microporous hollow fiber membranes, J. Membr. Sci. 369 (2011) 329–338, https://doi.org/10.1016/j.memsci.2010.12.008.
[63] M. Sangeetha, A. Mallikarjun, Y. Aparna, et al., Dielectric studies and AC conductivity of PVDF-HFP: LiBF4: EC plasticized polymer electrolytes, Mater. Today Proc. 44 (2021) 2168–2172, https://doi.org/10.1016/j.matpr.2020.12.280.
[64] Y. Li, W. Zhang, Q. Dou, et al., Li7La3Zr2O12 ceramic nanofiber-incorporated composite polymer electrolytes for lithium metal batteries, J Mater Chem A Mater 7 (2019) 3391–3398, https://doi.org/10.1039/C8TA11449H.
[65] S. Das, A. Ghosh, Charge carrier relaxation in different plasticized PEO/PVDF-HFP blend solid polymer electrolytes, J. Phys. Chem. B 121 (2017) 5422–5432, https://doi.org/10.1021/acs.jpcb.7b02277.
[66] A. Subramania, N.T.K. Sundaram, G.V. Kumar, Structural and electrochemical properties of micro-porous polymer blend electrolytes based on PVdF-co-HFP-PAN for Li-ion battery applications, J. Power Sources 153 (2006) 177–182, https://doi.org/10.1016/j.jpowsour.2004.12.009.
[67] H. Guo, S. Zhong, L. Chen, et al., Study on PVDF-HFP/PMMA/CMC blended polymer as membrane for lithium-ion batteries, Int. J. Electrochem. Sci. 17 (2022), https://doi.org/10.20964/2022.01.47.
[68] K.S. Ngai, S. Ramesh, K. Ramesh, J.C. Juan, A review of polymer electrolytes: fundamental, approaches and applications, Ionics 22 (2016) 1259–1279, https://doi.org/10.1007/s11581-016-1756-4.
[69] D. Chen, Y. Liu, C. Feng, et al., Unified throughout-pore microstructure enables ultrahigh separator porosity for robust high-flux lithium batteries, Electron 1 (2023), https://doi.org/10.1002/elt2.1.
[70] D. Zhang, X. Meng, W. Hou, et al., Solid polymer electrolytes: ion conduction mechanisms and enhancement strategies, Nano Research Energy 2 (2023) e9120050, https://doi.org/10.26599/NRE.2023.9120050.
[71] K.M. Kim, N.-G. Park, K.S. Ryu, S.H. Chang, Characteristics of PVdF-HFP/TiO2 composite membrane electrolytes prepared by phase inversion and conventional casting methods, Electrochim. Acta 51 (2006) 5636–5644, https://doi.org/10.1016/j.electacta.2006.02.038.
[72] D. Song, C. Xu, Y. Chen, et al., Enhanced thermal and electrochemical properties of PVDF-HFP/PMMA polymer electrolyte by TiO2 nanoparticles, Solid State Ionics 282 (2015) 31–36, https://doi.org/10.1016/j.ssi.2015.09.017.
[73] S. Caimi, A. Klaue, H. Wu, M. Morbidelli, Effect of SiO2 nanoparticles on the performance of PVdF-HFP/ionic liquid separator for lithium-ion batteries, Nanomaterials 8 (2018) 926, https://doi.org/10.3390/nano8110926.
[74] X. Yu, A. Manthiram, A review of composite polymer-ceramic electrolytes for lithium batteries, Energy Storage Mater. 34 (2021) 282–300, https://doi.org/10.1016/j.ensm.2020.10.006.
[75] A.M. Stephan, K.S. Nahm, M. Anbu Kulandainathan, et al., Poly(vinylidene fluoride-hexafluoropropylene) (PVdF-HFP) based composite electrolytes for lithium batteries, Eur. Polym. J. 42 (2006) 1728–1734, https://doi.org/10.1016/j.eurpolymj.2006.02.006.
[76] L. Tian, A. Li, Q. Huang, et al., Homogenously dispersed ultrasmall niobium(V) oxide nanoparticles enabling improved ionic conductivity and interfacial compatibility of composite polymer electrolyte, J. Colloid Interface Sci. 586 (2021) 855–865, https://doi.org/10.1016/j.jcis.2020.11.010.
[77] J. Pan, P. Zhao, H. Yao, et al., Inert filler selection strategies in Li-ion gel polymer electrolytes, ACS Appl. Mater. Interfaces (2023), https://doi.org/10.1021/acsami.3c05105.

[78] Y. Li, W. Zhang, Q. Dou, et al., $Li_7La_3Zr_2O_{12}$ ceramic nanofiber-incorporated composite polymer electrolytes for lithium metal batteries, J Mater Chem A Mater 7 (2019) 3391–3398, https://doi.org/10.1039/C8TA11449H.

[79] Y. Wang, T. Liu, C. Liu, et al., Solid-state lithium battery with garnet Li7La3Zr2O12 nanofibers composite polymer electrolytes, Solid State Ionics 378 (2022), https://doi.org/10.1016/j.ssi.2022.115897.

[80] K. Liu, M. Wu, L. Wei, et al., A composite solid electrolyte with a framework of vertically aligned perovskite for all-solid-state Li-metal batteries, J. Membr. Sci. 610 (2020), https://doi.org/10.1016/j.memsci.2020.118265.

[81] Z. Luo, W. Li, C. Guo, et al., Two-dimensional silica enhanced solid polymer electrolyte for lithium metal batteries, Particuology 85 (2024) 146–154, https://doi.org/10.1016/j.partic.2023.04.002.

[82] M. Yao, T. Yu, Q. Ruan, et al., High-voltage and wide-temperature lithium metal batteries enabled by ultrathin MOF-derived solid polymer electrolytes with modulated ion transport, ACS Appl. Mater. Interfaces 13 (2021) 47163–47173, https://doi.org/10.1021/acsami.1c15038.

[83] W. Wieczorek, K. Such, H. Wyci~Lik, J. Plocharski, Modifications of crystalline structure of PEO polymer electrolytes with ceramic additives, Solid State Ionics 36 (1989) 255–257.

[84] P. Senthil Kumar, A. Sakunthala, K. Govindan, et al., Single crystalline TiO2 nanorods as effective fillers for lithium ion conducting PVdF-HFP based composite polymer electrolytes, RSC Adv. 6 (2016) 91711–91719, https://doi.org/10.1039/c6ra20649b.

[85] N. Angulakshmi, S. Thomas, K.S. Nahm, et al., Electrochemical and mechanical properties of nanochitin-incorporated PVDF-HFP-based polymer electrolytes for lithium batteries, Ionics 17 (2011) 407–414, https://doi.org/10.1007/s11581-010-0517-z.

[86] W. Xiong, T. Huang, Y. Feng, et al., Rapid ionic conductivity of ternary composite electrolytes for superior solid-state batteries with high-rate performance and long cycle life operated at room temperature, J Mater Chem A Mater 9 (2021) 18338–18348, https://doi.org/10.1039/d1ta05751k.

[87] J. Cao, L. Wang, M. Fang, et al., Structure and electrochemical properties of composite polymer electrolyte based on poly vinylidene fluoride-hexafluoropropylene/titania-poly(methyl methacrylate) for lithium-ion batteries, J. Power Sources 246 (2014) 499–504, https://doi.org/10.1016/j.jpowsour.2013.07.107.

[88] P. Vickraman, V. Senthilkumar, A study on the role of $BaTiO_3$ in lithum bis (perfluoroethanesulfonyl)imide-based PVDF-HFP nanocomposites, Ionics 16 (2010) 763–768, https://doi.org/10.1007/s11581-010-0467-5.

[89] Z. Li, X. Wang, X. Lin, et al., Ferroelectric nanorods as a polymer interface additive for high-performance garnet-based solid-state batteries, ACS Appl. Mater. Interfaces 15 (2023) 35684–35691, https://doi.org/10.1021/acsami.3c06095.

[90] M. Sasikumar, M. Raja, R.H. Krishna, et al., Influence of hydrothermally synthesized cubic-structured $BaTiO_3$ ceramic fillers on ionic conductivity, mechanical integrity, and thermal behavior of P(VDF-HFP)/PVAc-based composite solid polymer electrolytes for lithium-ion batteries, J. Phys. Chem. C 122 (2018) 25741–25752, https://doi.org/10.1021/acs.jpcc.8b03952.

[91] T. Wei, Z hong Zhang, Q. Zhang, et al., Anion-immobilized solid composite electrolytes based on metal-organic frameworks and superacid ZrO_2 fillers for high-performance all solid-state lithium metal batteries, Int. J. Miner. Metall. Mater. 28 (2021) 1636–1646, https://doi.org/10.1007/s12613-021-2289-z.

[92] Y. Ji, B. Yuan, J. Zhang, et al., A single-layer piezoelectric composite separator for durable operation of Li metal anode at high rates, Energy and Environmental Materials (2022), https://doi.org/10.1002/eem2.12510.

[93] V.R. Sunitha, S. Radhakrishnan, Field enhanced Li ion conduction in nanoferroelectric modified polymer electrolyte systems, Ionics 21 (2015) 949–954, https://doi.org/10.1007/s11581-014-1252-7.

[94] J.C. Barbosa, R. Gonçalves, C.M. Costa, et al., Metal–organic frameworks and zeolite materials as active fillers for lithium-ion battery solid polymer electrolytes, Mater Adv 2 (2021) 3790–3805, https://doi.org/10.1039/D1MA00244A.

[95] S. Cui, X. Wu, Y. Yang, et al., Heterostructured gel polymer electrolyte enabling long-cycle quasi-solid-state lithium metal batteries, ACS Energy Lett. 7 (2022) 42–52, https://doi.org/10.1021/acsenergylett.1c02233.

[96] L. Liu, C. Sun, Flexible quasi-solid-state composite electrolyte membrane derived from a metal-organic framework for lithium-metal batteries, Chemelectrochem 7 (2020) 707–715, https://doi.org/10.1002/celc.201902032.

[97] A. Corma, From microporous to mesoporous molecular sieve materials and their use in catalysis, Chem. Rev. 97 (1997) 2373–2420, https://doi.org/10.1021/cr960406n.

[98] W. Xiao, X. Li, Z. Wang, H. Guo, Study on performances of ZSM-5 doped P(VDF-HFP) based composite polymer electrolyte prepared by steam bath technique, Iranian Polymer Journal (English Edition 21 (2012) 481–488, https://doi.org/10.1007/s13726-012-0052-z.

[99] Y.X. Jiang, Z.F. Chen, Q.C. Zhuang, et al., A novel composite microporous polymer electrolyte prepared with molecule sieves for Li-ion batteries, J. Power Sources 160 (2006) 1320–1328, https://doi.org/10.1016/j.jpowsour.2006.02.029.

[100] A.K. Solarajan, V. Murugadoss, S. Angaiah, Montmorillonite embedded electrospun PVdF–HFP nanocomposite membrane electrolyte for Li-ion capacitors, Appl. Mater. Today 5 (2016) 33–40, https://doi.org/10.1016/j.apmt.2016.09.002.

[101] L. Zhang, X. Xu, S. Jiang, et al., Halloysite nanotubes modified poly (vinylidenefluoride-co-hexafluoropropylene)-based polymer-in-salt electrolyte to achieve high-performance Li metal batteries, J. Colloid Interface Sci. 645 (2023) 45–54, https://doi.org/10.1016/j.jcis.2023.04.127.

[102] Y. Zeng, L. Zhao, J. Zhang, et al., La_2O_3 filler's stabilization of residual solvent in polymer electrolyte for advanced solid-state lithium-metal batteries, Small Science 3 (2023), https://doi.org/10.1002/smsc.202300017.

[103] S. Aadheeshwaran, K. Sankaranarayanan, Electrochemical behavior of $BaTiO_3$ embedded spongy PVDF-HFP/cellulose blend as a novel gel polymer electrolyte for lithium-ion batteries, Mater. Lett. 306 (2022), https://doi.org/10.1016/j.matlet.2021.130938.

[104] M. Yao, T. Yu, Q. Ruan, et al., High-voltage and wide-temperature lithium metal batteries enabled by ultrathin MOF-derived solid polymer electrolytes with modulated ion transport, ACS Appl. Mater. Interfaces 13 (2021) 47163–47173, https://doi.org/10.1021/acsami.1c15038.

[105] J. Li, L. Zhu, H. Xie, et al., Graphitic carbon nitride assisted PVDF-HFP based solid electrolyte to realize high performance solid-state lithium metal batteries, Colloids Surf. A Physicochem. Eng. Asp. 657 (2023), https://doi.org/10.1016/j.colsurfa.2022.130520.

[106] P. Zhai, Z. Yang, Y. Wei, et al., Two-dimensional fluorinated graphene reinforced solid polymer electrolytes for high-performance solid-state lithium batteries, Adv. Energy Mater. 12 (2022), https://doi.org/10.1002/aenm.202200967.

[107] J. Li, L. Zhu, H. Xie, et al., Graphitic carbon nitride assisted PVDF-HFP based solid electrolyte to realize high performance solid-state lithium metal batteries, Colloids Surf. A Physicochem. Eng. Asp. 657 (2023), https://doi.org/10.1016/j.colsurfa.2022.130520.

[108] W. Xiao, X. Li, H. Guo, et al., Preparation and physicochemical performances of poly[(vinylidene fluoride)-co-hexafluoropropylene]-based composite polymer electrolytes doped with modified carbon nanotubes, Polym. Int. 63 (2014) 307–314, https://doi.org/10.1002/pi.4506.

[109] J. Li, L. Zhu, J. Zhang, et al., Approaching high performance PVDF-HFP based solid composite electrolytes with LLTO nanorods for solid-state lithium-ion batteries, Int. J. Energy Res. 45 (2021) 7663–7674, https://doi.org/10.1002/er.6347.

[110] M. Morales, Phase diagram, crystal chemistry and lithium ion conductivity in the perovskite-type system $Pr_{0,\ 5+x}Li_{0.5-3x}TiO_3$. Solid State Ion 91 (1996) 33–43, https://doi.org/10.1016/S0167-2738(96)00420-1.

[111] Y. Inaguma, J. Yu, Y. Shan, et al., The effect of the hydrostatic pressure on the ionic conductivity in a perovskite lanthanum lithium titanate, J. Electrochem. Soc. 142 (1995), https://doi.org/10.1149/1.2043988. L8–L11.

[112] H. Kawai, J. Kuwano, Lithium ion conductivity of A-site deficient perovskite solid solution $La_{0.67\ -\ x}Li_{3x}TiO_3$, J. Electrochem. Soc. 141 (1994) L78–L79, https://doi.org/10.1149/1.2055043.

[113] H. Yang, K. Tay, Y. Xu, et al., Nitrogen-doped lithium lanthanum titanate nanofiber-polymer composite electrolytes for all-solid-state lithium batteries, J. Electrochem. Soc. 168 (2021) 110507, https://doi.org/10.1149/1945-7111/ac30ad.

[114] H.T.T. Le, D.T. Ngo, R.S. Kalubarme, et al., Composite gel polymer electrolyte based on poly(vinylidene fluoride-hexafluoropropylene) (PVDF-HFP) with modified aluminum-doped lithium lanthanum titanate (A-LLTO) for high-performance lithium rechargeable batteries, ACS Appl. Mater. Interfaces 8 (2016) 20710–20719, https://doi.org/10.1021/acsami.6b05301.

[115] L. Zhu, H. Xie, W. Zheng, K. Zhang, Multi-component solid PVDF-HFP/PPC/LLTO-nanorods composite electrolyte enabling advanced solid-state lithium metal batteries, Electrochim. Acta 435 (2022), https://doi.org/10.1016/j.electacta.2022.141384.

[116] Y. Li, W. Arnold, A. Thapa, et al., Stable and flexible sulfide composite electrolyte for high-performance solid-state lithium batteries, ACS Appl. Mater. Interfaces 12 (2020) 42653–42659, https://doi.org/10.1021/acsami.0c08261.

[117] R. Murugan, V. Thangadurai, W. Weppner, Fast lithium ion conduction in garnet-type Li7La3Zr2O12, Angew. Chem. Int. Ed. 46 (2007) 7778–7781, https://doi.org/10.1002/anie.200701144.

[118] A. Kim, J.-H. Kang, K. Song, B. Kang, Simultaneously improved cubic phase stability and Li-ion conductivity in garnet-type solid electrolytes enabled by controlling the Al occupation sites, ACS Appl. Mater. Interfaces 14 (2022) 12331–12339, https://doi.org/10.1021/acsami.2c01361.

[119] Y. Li, W. Zhang, Q. Dou, et al., $Li_7La_3Zr_2O_{12}$ ceramic nanofiber-incorporated composite polymer electrolytes for lithium metal batteries, J Mater Chem A Mater 7 (2019) 3391–3398, https://doi.org/10.1039/c8ta11449h.

[120] S.L. Beshahwured, Y.S. Wu, S huang Wu, et al., Flexible hybrid solid electrolyte incorporating ligament-shaped $Li_{6.25}Al_{0.25}La_3Zr_2O_{12}$ filler for all-solid-state lithium-metal batteries, Electrochim. Acta 366 (2021), https://doi.org/10.1016/j.electacta.2020.137348.

[121] J. Zhang, N. Zhao, M. Zhang, et al., Flexible and ion-conducting membrane electrolytes for solid-state lithium batteries: dispersion of garnet nanoparticles in insulating polyethylene oxide, Nano Energy 28 (2016) 447–454, https://doi.org/10.1016/j.nanoen.2016.09.002.

[122] Y. Xu, K. Wang, Y. An, et al., Rapid ion transport induced by the enhanced interaction in composite polymer electrolyte for all-solid-state lithium-metal batteries, J. Phys. Chem. Lett. 12 (2021) 10603–10609, https://doi.org/10.1021/acs.jpclett.1c02701.

[123] S. Tao, J. Li, L. Wang, et al., Coral-like $Li_7La_3Zr_2O_{12}$-filled PVDF-HFP/LiODFB composite electrolytes for solid-state batteries with excellent cycle performance, ACS Appl. Energy Mater. 4 (2021) 11447–11459, https://doi.org/10.1021/acsaem.1c02217.

[124] J. Sun, X. Yao, Y. Li, et al., Facilitating interfacial stability via bilayer heterostructure solid electrolyte toward high-energy, safe and adaptable lithium

batteries, Adv. Energy Mater. 10 (2020), https://doi.org/10.1002/aenm.202000709.
[125] H. Huo, Y. Chen, J. Luo, et al., Rational design of hierarchical "ceramic-in-polymer" and "polymer-in-ceramic" electrolytes for dendrite-free solid-state batteries, Adv. Energy Mater. 9 (2019) 1804004, https://doi.org/10.1002/aenm.201804004.
[126] Q. Zhang, D. Cao, Y. Ma, et al., Sulfide-based solid-state electrolytes: synthesis, stability, and potential for all-solid-state batteries, Adv. Mater. 31 (2019) 1901131, https://doi.org/10.1002/adma.201901131.
[127] F. Han, Y. Zhu, X. He, et al., Electrochemical stability of $Li_{10}GeP_2S_{12}$ and $Li_7La_3Zr_2O_{12}$ solid electrolytes, Adv. Energy Mater. 6 (2016) 1501590, https://doi.org/10.1002/aenm.201501590.
[128] L. Cong, Y. Li, W. Lu, et al., Unlocking the Poly(vinylidene fluoride-co-hexafluoropropylene)/Li10GeP2S12 composite solid-state Electrolytes for Dendrite-Free Li metal batteries assisting with perfluoropolyethers as bifunctional adjuvant, J. Power Sources 446 (2020), https://doi.org/10.1016/j.jpowsour.2019.227365.
[129] S.D. Tao, J. Li, R. Hu, et al., $3Li_2S$-$2MoS_2$ filled composite polymer PVDF-HFP/LiODFB electrolyte with excellent interface performance for lithium metal batteries, Appl. Surf. Sci. 536 (2021), https://doi.org/10.1016/j.apsusc.2020.147794.
[130] P. Zhang, M. Matsui, Y. Takeda, et al., Water-stable lithium ion conducting solid electrolyte of iron and aluminum doped NASICON-type $LiTi_2(PO_4)_3$, Solid State Ionics 263 (2014) 27–32, https://doi.org/10.1016/j.ssi.2014.04.017.
[131] Y. Liu, B. Li, H. Kitaura, et al., Fabrication and performance of all-solid-state Li–air battery with SWCNTs/LAGP cathode, ACS Appl. Mater. Interfaces 7 (2015) 17307–17310, https://doi.org/10.1021/acsami.5b04409.
[132] B. Key, D.J. Schroeder, B.J. Ingram, J.T. Vaughey, Solution-based synthesis and characterization of lithium-ion conducting phosphate ceramics for lithium metal batteries, Chem. Mater. 24 (2012) 287–293, https://doi.org/10.1021/cm202773d.
[133] A. Cassel, B. Fleutot, M. Courty, et al., Sol-gel synthesis and electrochemical properties extracted by phase inflection detection method of NASICON-type solid electrolytes $LiZr_2(PO_4)_3$ and $Li_{1.2}Zr_{1.9}Ca_{0.1}(PO_4)_3$, Solid State Ionics 309 (2017) 63–70, https://doi.org/10.1016/j.ssi.2017.07.009.
[134] Y. Nikodimos, M.-C. Tsai, L.H. Abrha, et al., Al–Sc dual-doped $LiGe_2(PO_4)_3$ – a NASICON-type solid electrolyte with improved ionic conductivity, J Mater Chem A Mater 8 (2020) 11302–11313, https://doi.org/10.1039/D0TA00517G.
[135] H. Morimoto, H. Awano, J. Terashima, et al., Preparation of lithium ion conducting solid electrolyte of NASICON-type $Li_{1+x}Al_xTi_{2-x}(PO_4)_3$ (x = 0.3) obtained by using the mechanochemical method and its application as surface modification materials of $LiCoO_2$ cathode for lithium cell, J. Power Sources 240 (2013) 636–643, https://doi.org/10.1016/j.jpowsour.2013.05.039.
[136] O.L. Andreev, K.V. Druzhinin, P.Y. Shevelin, N.N. Batalov, Influence of solid electrolyte particles size on ionic transport in model composite system (PVdF-HFP-$Li_{1.3}Al_{0.3}Ti_{1.7}(PO_4)_3$), Ionics 19 (2013) 33–39, https://doi.org/10.1007/s11581-012-0706-z.
[137] Y. Li, H. Wang, Composite solid electrolytes with NASICON-type LATP and PVdF-HFP for solid-state lithium batteries, Ind. Eng. Chem. Res. 60 (2021) 1494–1500, https://doi.org/10.1021/acs.iecr.0c05075.
[138] H. Yang, K. Tay, Y. Xu, et al., Nitrogen-doped lithium lanthanum titanate nanofiber-polymer composite electrolytes for all-solid-state lithium batteries, J. Electrochem. Soc. 168 (2021) 110507, https://doi.org/10.1149/1945-7111/ac30ad.
[139] X. Zhou, H. Jiang, H. Zheng, et al., Nonflammable hybrid solid electrolyte membrane for a solid-state lithium battery compatible with conventional porous electrodes, J. Membr. Sci. 603 (2020), https://doi.org/10.1016/j.memsci.2020.117820.
[140] Y. Jin, X. Zong, X. Zhang, et al., Constructing 3D Li+-percolated transport network in composite polymer electrolytes for rechargeable quasi-solid-state lithium batteries, Energy Storage Mater. 49 (2022) 433–444, https://doi.org/10.1016/j.ensm.2022.04.035.
[141] L. Cong, Y. Li, W. Lu, et al., Unlocking the Poly(vinylidene fluoride-co-hexafluoropropylene)/$Li_{10}GeP_2S_{12}$ composite solid-state Electrolytes for Dendrite-Free Li metal batteries assisting with perfluoropolyethers as bifunctional adjuvant, J. Power Sources 446 (2020), https://doi.org/10.1016/j.jpowsour.2019.227365.
[142] Q. Zhang, Q. Wang, S. Huang, et al., Preparation and electrochemical study of PVDF-HFP/LATP/g-C_3N_4 composite polymer electrolyte membrane, Inorg. Chem. Commun. 131 (2021), https://doi.org/10.1016/j.inoche.2021.108793.
[143] R. Xu, X.Q. Zhang, X.B. Cheng, et al., Artificial soft–rigid protective layer for dendrite-free lithium metal anode, Adv. Funct. Mater. 28 (2018), https://doi.org/10.1002/adfm.201705838.
[144] L. Cong, Y. Li, W. Lu, et al., Unlocking the Poly(vinylidene fluoride-co-hexafluoropropylene)/$Li_{10}GeP_2S_{12}$ composite solid-state Electrolytes for Dendrite-Free Li metal batteries assisting with perfluoropolyethers as bifunctional adjuvant, J. Power Sources 446 (2020), https://doi.org/10.1016/j.jpowsour.2019.227365.
[145] P. Senthil Kumar, A. Sakunthala, K. Govindan, et al., Single crystalline TiO_2 nanorods as effective fillers for lithium ion conducting PVdF-HFP based composite polymer electrolytes, RSC Adv. 6 (2016) 91711–91719, https://doi.org/10.1039/c6ra20649b.
[146] M. Sasikumar, M. Raja, R.H. Krishna, et al., Influence of hydrothermally synthesized cubic-structured $BaTiO_3$ ceramic fillers on ionic conductivity, mechanical integrity, and thermal behavior of P(VDF-HFP)/PVAc-based composite solid polymer electrolytes for lithium-ion batteries, J. Phys. Chem. C 122 (2018) 25741–25752, https://doi.org/10.1021/acs.jpcc.8b03952.
[147] L. Yi, C. Zou, X. Chen, et al., One-step synthesis of PVDF-HFP/PMMA-ZrO_2 gel polymer electrolyte to boost the performance of a lithium metal battery, ACS Appl. Energy Mater. 5 (2022) 7317–7327, https://doi.org/10.1021/acsaem.2c00831.
[148] S. Xia, B. Yang, H. Zhang, et al., Ultrathin layered double hydroxide nanosheets enabling composite polymer electrolyte for all-solid-state lithium batteries at room temperature, Adv. Funct. Mater. 31 (2021), https://doi.org/10.1002/adfm.202101168.
[149] L. Tian, F. Tao, X. Wang, et al., Efficient improvement of the lithium ionic conductivity for a polymer electrolyte via introducing porous metal-organic frameworks, Chem. Commun. 58 (2022) 6717–6720, https://doi.org/10.1039/d2cc01458k.
[150] P. Xu, H. Chen, X. Zhou, H. Xiang, Gel polymer electrolyte based on PVDF-HFP matrix composited with rGO-PEG-NH2 for high-performance lithium-ion battery, J. Membr. Sci. 617 (2021), https://doi.org/10.1016/j.memsci.2020.118660.
[151] Z. Zhang, R.G. Antonio, K.L. Choy, Boron nitride enhanced polymer/salt hybrid electrolytes for all-solid-state lithium-ion batteries, J. Power Sources 435 (2019), https://doi.org/10.1016/j.jpowsour.2019.226736.
[152] K. Huang, Y. Wang, H. Mi, et al., BF_4-modified PVDF-HFP composite polymer electrolyte for high-performance solid-state lithium metal battery, J Mater Chem A Mater 8 (2020) 20593–20603, https://doi.org/10.1039/d0ta08169h.
[153] L. Zhu, H. Xie, W. Zheng, K. Zhang, Multi-component solid PVDF-HFP/PPC/LLTO-nanorods composite electrolyte enabling advanced solid-state lithium metal batteries, Electrochim. Acta 435 (2022), https://doi.org/10.1016/j.electacta.2022.141384.
[154] A. Das, M. Goswami, K. Illath, et al., Synthesis and characterization of LAGP-glass-ceramics-based composite solid polymer electrolyte for solid-state Li-ion battery application, J. Non-Cryst. Solids 558 (2021), https://doi.org/10.1016/j.jnoncrysol.2021.120654.
[155] S.L. Beshahwured, T.H. Mengesha, L.M. Babulal, Y-S. Wu, S-H. Wu, J-K. Chang, R. Jose, C-C Yang, Hierarchical Interconnected Hybrid Solid Electrolyte Membrane for All-Solid-State Lithium-Metal Batteries Based on High-Voltage NCM811 CathodesFlexible hybrid solid electrolyte incorporating ligament-shaped $Li_{6.25}Al_{0.25}La_3Zr_2O_{12}$ filler for all-solid-state lithium-metal batteries, ACS Appl. Energy Mater. 5 (2) (2022) 2580–2595, https://doi.org/10.1021/acsaem.2c00046.
[156] H. Yang, K. Tay, Y. Xu, et al., Nitrogen-doped lithium lanthanum titanate nanofiber-polymer composite electrolytes for all-solid-state lithium batteries, J. Electrochem. Soc. 168 (2021) 110507, https://doi.org/10.1149/1945-7111/ac30ad.
[157] T. Huang, W. Xiong, X. Ye, et al., A cerium-doped NASICON chemically coupled poly(vinylidene fluoride-hexafluoropropylene)-based polymer electrolyte for high-rate and high-voltage quasi-solid-state lithium metal batteries, J. Energy Chem. 73 (2022) 311–321, https://doi.org/10.1016/j.jechem.2022.06.030.
[158] J. Lu, Y. Liu, P. Yao, et al., Hybridizing poly(vinylidene fluoride-co-hexafluoropropylene) with $Li_{6.5}La_3Zr_{1.5}Ta_{0.5}O_{12}$ as a lithium-ion electrolyte for solid state lithium metal batteries, Chem. Eng. J. 367 (2019) 230–238, https://doi.org/10.1016/j.cej.2019.02.148.
[159] S.D. Tao, J. Li, R. Hu, et al., $3Li_2S$-$2MoS_2$ filled composite polymer PVDF-HFP/LiODFB electrolyte with excellent interface performance for lithium metal batteries, Appl. Surf. Sci. 536 (2021), https://doi.org/10.1016/j.apsusc.2020.147794.
[160] Y. Li, W. Zhang, Q. Dou, et al., $Li_7La_3Zr_2O_{12}$ ceramic nanofiber-incorporated composite polymer electrolytes for lithium metal batteries, J Mater Chem A Mater 7 (2019) 3391–3398, https://doi.org/10.1039/c8ta11449h.
[161] Y. Li, W. Arnold, A. Thapa, et al., Stable and flexible sulfide composite electrolyte for high-performance solid-state lithium batteries, ACS Appl. Mater. Interfaces 12 (2020) 42653–42659, https://doi.org/10.1021/acsami.0c08261.
[162] S.Y. Du, G.X. Ren, N. Zhang, X.S. Liu, High-performance poly(vinylidene fluoride-hexafluoropropylene)-Based composite electrolytes with excellent interfacial compatibility for room-temperature all-solid-state lithium metal batteries, ACS Omega 7 (2022) 19631–19639, https://doi.org/10.1021/acsomega.2c01338.
[163] J. Ma, H. Jiang, L. Chen, et al., Interfacial optimization between cathode and 20 μm-thickness solid electrolyte membrane via in-situ polymerization for lithium metal batteries, J. Power Sources 537 (2022), https://doi.org/10.1016/j.jpowsour.2022.231517.
[164] H.K. Tran, B.T. Truong, B.R. Zhang, et al., Sandwich-structured composite polymer electrolyte based on PVDF-HFP/PPC/Al-doped LLZO for high-voltage solid-state lithium batteries, ACS Appl. Energy Mater. 6 (2023) 1475–1487, https://doi.org/10.1021/acsaem.2c03363.